15
Geochemical Tracers and Ocean Circulation

W. S. Broecker

15.1 Introduction

Tracers have always been an important adjunct to physical oceanography. The distribution of dissolved oxygen (and to some extent of the nutrients, nitrate, phosphate, and silica) played a very important role in defining the major water masses of the ocean [see Sverdrup, Johnson, and Fleming (1942) for a review of this subject]. Many attempts also have been made to harness the loss of dissolved oxygen from the water column as a measure of the rates of oceanic mixing processes (e.g., Riley, 1951; Wyrtki, 1962). These latter pursuits, however, have been of only marginal success because of our lack of knowledge of the consumption rate of O_2 within the sea.

The big breakthrough in geochemical tracing came after World War II with the discovery of the cosmic-ray-produced isotopes ^{14}C and ^{3}H. A further impetus to this field came with the realization in the mid 1950s that the ocean was receiving significant amounts of ^{90}Sr, ^{137}Cs, ^{3}H, ^{14}C, etc., from nuclear testing. Because the distributions of radioisotopes offered information not so highly dependent on assumptions regarding the rates at which biological processes proceed in the ocean, the emphasis in chemical oceanography moved quickly away from the traditional chemical tracers to the radiotracers. Only quite recently has interest in the chemically used compounds in the sea been renewed. Three reasons can be given for this renaissance:

(1) Radiocarbon is transported in particulate matter as well as in solution; hence the contributions of the two processes must be separated if the distribution of ^{14}C is to be used for water-transport modeling. This separation is based on the distribution of ΣCO_2 (concentration of total dissolved inorganic carbon), alkalinity, and dissolved O_2 in the ocean.

(2) The concentrations of nitrate and phosphate can be combined with that of dissolved oxygen to yield the quasi-conservative properties "PO" and "NO". As reviewed below, such properties are needed in modeling to unscramble the "mixtures" found in the deep sea.

(3) With the advent of (a) sediment trapping and other means for the direct measurement of the fluxes of particulate matter into the deep sea, (b) devices designed to measure the fluxes of materials from the sea floor, and (c) better means for the measurement of plant productivity, interest has been renewed in generating models capable of simultaneously explaining the distribution of the chemical species, the distribution of the radiospecies, and the flux measurements.

In this chapter I shall emphasize the development of radioisotope tracing, as I feel that it constitutes the major contribution of geochemistry to our understanding of ocean circulation over the past four decades (i.e., since the writing of *The Oceans*). I will mention the

use of the classical chemical tracers only where they bear on the interpretation of the radioisotope data.

Over the last decade, the Geochemical Ocean Sections Study (GEOSECS) has determined the distribution of the radioisotope tracers on a global scale. Attempts to model the previously existing ^{14}C results (Bolin and Stommel, 1961; Arons and Stommel, 1967) made clear the inadequacy of this data set. Henry Stommel therefore brought together a number of geochemists interested in this problem, and encouraged them to think big, to work together, and to produce a global set of very accurate ^{14}C data.

Because of its massive scope and of the measurement accuracy achieved, the GEOSECS data set has become dominant in the field of marine geochemistry. While previously existing radioisotope data (for review see Burton, 1975) were of great importance in the development of thinking with regard to the interpretation of tracer results and in the separation of the natural and the bomb-test contributions to ^{14}C and ^{3}H, the new data set eclipses what we had in 1969 when this program began. Thus I shall refer frequently to these new results in the sections that follow.

At the time this chapter was written the GEOSECS field program had been completed. Maps showing the ship tracks and station positions are given in figure 15.1. The laboratory analyses for the Atlantic and Pacific phases of the program are complete. Those for the Indian Ocean are still in progress. The mammoth job of making scientific use of this data set has just begun. Many years will pass before the meat of this effort will appear in print.

15.2 Water-Transport Tracers

The efforts in the field of radioisotope tracing can be divided into two categories: those that are aimed at a better understanding of the dynamics of the ventilation of, and mixing within, the ocean's interior, and those that are aimed at a better understanding of the origin, movement, and fate of particulate matter within the sea. While many of the tracers we use are influenced by both processes, a division can be made into a group primarily distributed by water transport and into a group primarily distributed by particulate transport (table 15.1). I will simplify my task by discussing here only the water-transport tracers.

The water-transport tracers can be subdivided according to their mode of origin. ^{90}Sr, ^{137}Cs, ^{85}Kr, and the freons are entirely anthropogenic in origin and hence are "transient tracers." ^{39}Ar, ^{222}Rn, ^{228}Ra, and ^{32}Si are entirely natural in origin and hence are steady-state tracers. ^{14}C and ^{3}H are in part natural and in part anthropogenic in origin. In the case of ^{3}H the man-made component dominates. For ^{14}C the man-made compo-

nent constitutes about 20% of the total in surface waters and is negligible in deep water.

^{3}He, the daughter product of ^{3}H, is also a tracer. It is produced within the sea by the decay of its parent; it also leaks into the deep sea from the mantle. These components produce an excess over atmospheric solubility within the sea. As will be shown below, the contributions of these sources can usually be separated.

The applicability of any given isotope depends on its half-life (in the case of steady-state tracers), or its temporal-input function (in the case of the transient tracers). It also depends on the geographic distribution of the input function. The differences from tracer to tracer are sufficiently large that the information obtained from the distribution of one isotope is not redundant with that obtained from another tracer. In the sections that follow the geochemistry of each of these tracers is reviewed.

Natural radiocarbon: ^{14}C is produced in the atmosphere by the interaction of ^{14}N atoms and the neutrons produced by cosmic rays. The current production rate is estimated to be about 2.2 atoms $cm^{-2}s^{-1}$ (Lingenfelter and Ramaty, 1970). This production is balanced by the beta decay of radiocarbon atoms. In its 8200-year mean lifetime, the average ^{14}C atom can penetrate the active carbon reservoirs (atmosphere, terrestrial biosphere, ocean, ice, soils). Some ^{14}C atoms become

Table 15.1 Ocean Tracers Currently in Use[a]

Isotope	Half-life (years)	Cosmic rays	U+Th series	Weapons testing	Other anthro.
^{14}C	5730	✓		✓	
^{226}Ra	1600		✓		
^{32}Si	250	✓			
^{39}Ar	270	✓			
^{137}Cs	30.2			✓	
^{90}Sr	28.6			✓	
^{3}H	12.4	✓		✓	
^{3}He	—	✓	✓	✓	
^{85}Kr	10.7			✓	✓
^{228}Ra	5.8		✓		
^{7}Be	0.15	✓			
^{222}Rn	0.01		✓		
Freons	—				✓
^{239}Pu	24,400			✓	✓
^{240}Pu	6540			✓	✓
^{210}Pb	22.3		✓		
^{228}Th	1.9		✓		
^{210}Po	0.38		✓		
^{234}Th	0.07		✓		

a. In the column headed Isotopes, freons and all entries above it are water tracers; all entries below freons are particulate tracers.
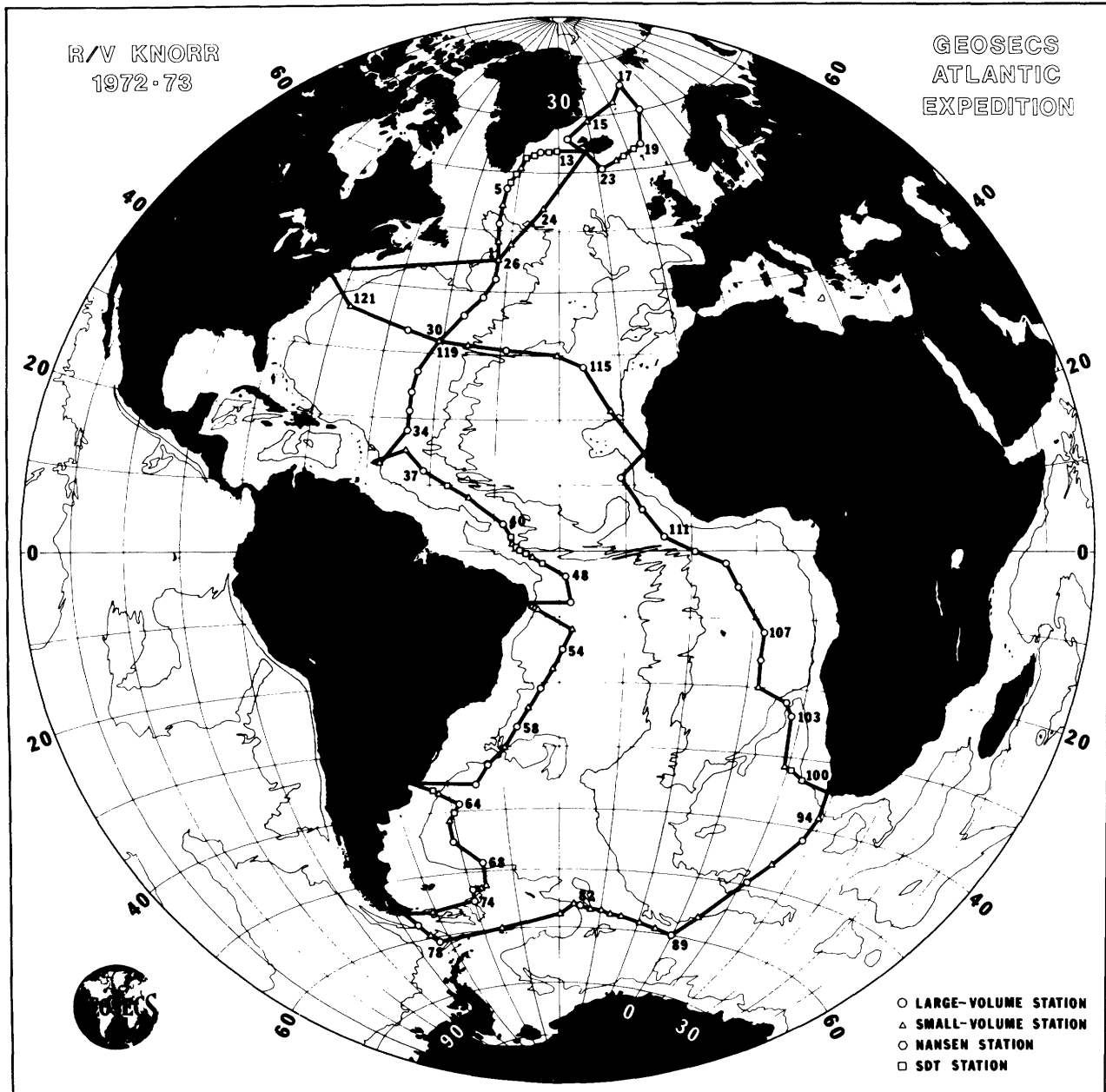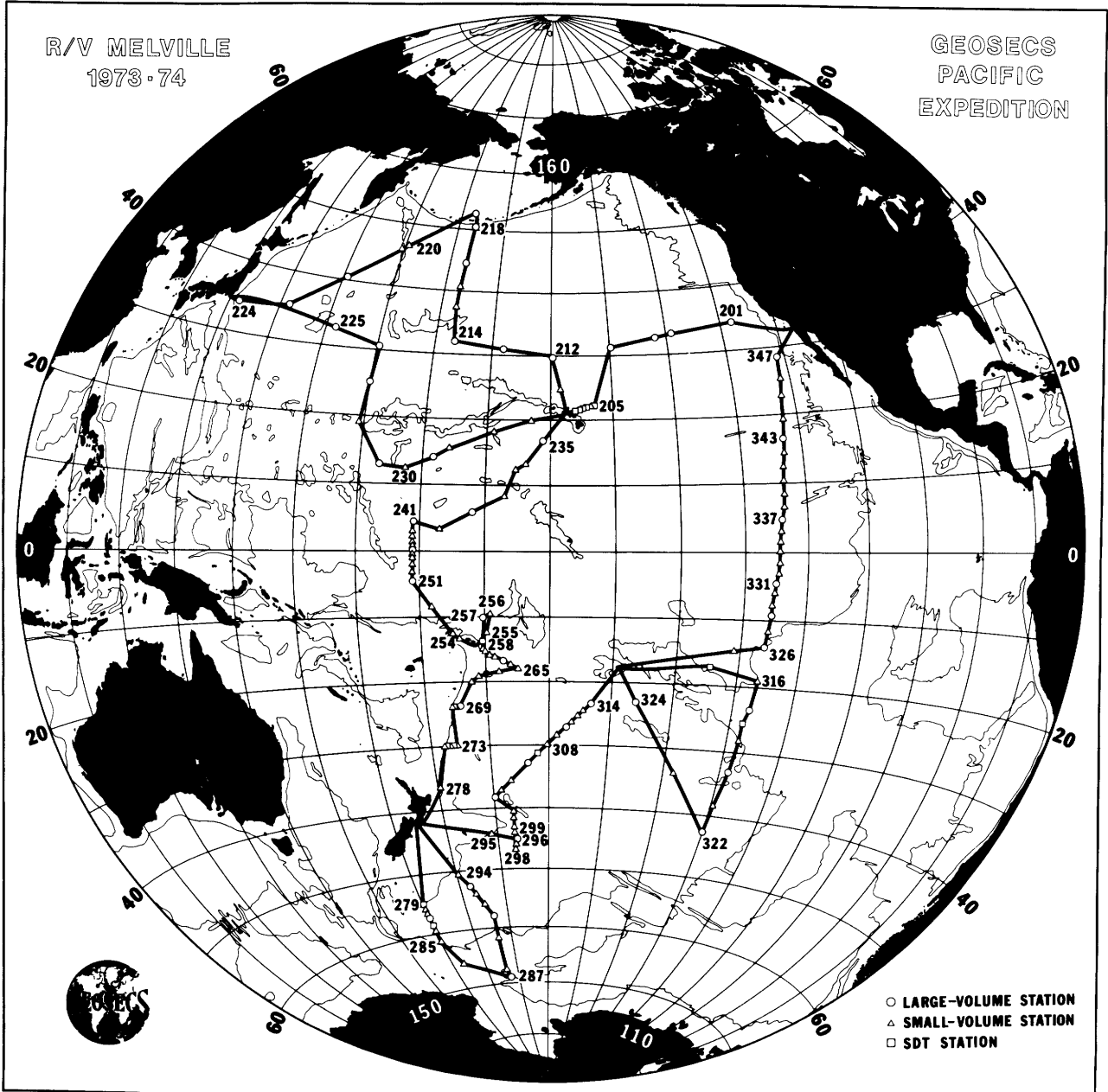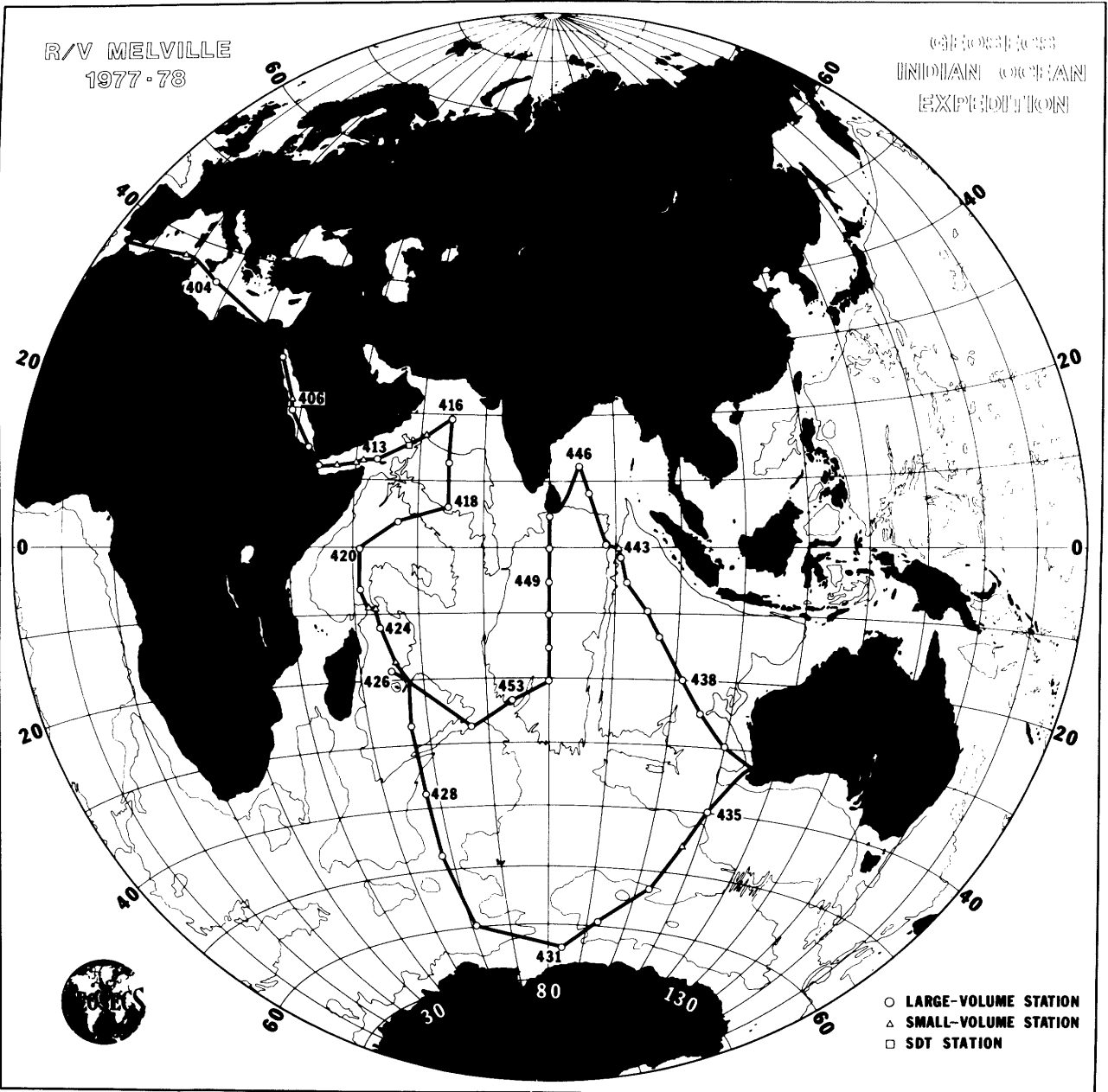
(15.1A)

Figure 15.1 Maps showing the locations of the stations occupied during the GEOSECS program in the Atlantic (A), Pacific (B), and Indian (C) Oceans. Those properties measurable on 30-liter samples were determined at every station. Radiocarbon, which requires ~250 liters of water, was sampled only at the large-volume stations. The 4000-m contour is shown on each map.

60

160

40

40

218
220

224
225
214
212
201

20
347
20

205
343
235

230
337
241

331
251

256
257
255
254
258
326
265
316
314
324
269
308
273
322
278

299
295
296
298
294
279
285
287

○ LARGE-VOLUME STATION
△ SMALL-VOLUME STATION
□ SDT STATION

60
150
110
60

GEOSECS

(15.1B)

bound into inactive reservoirs (e.g., marine sediments, peats) before their radiodemise. Table 15.2 summarizes the distribution of radiocarbon among these reservoirs.

Because of variability in the flux of cosmic rays, the production rate of ^{14}C has not remained constant with time. Also it is possible that the rates of the processes that distribute ^{14}C among the various reservoirs have changed with climate. Thus, as shown by measurements on tree rings (figure 15.2), the $^{14}C/C$ ratio in atmospheric CO_2 has not remained constant with time. As pointed out by Stuiver (1976), these variations must be considered when attempting to derive ventilation times from the distribution of ^{14}C within the sea.

During the present century the release of ^{14}C-free CO_2 to the atmosphere through the combustion of fossil fuels has measurably reduced the $^{14}C/C$ ratio. The decline between 1850 and 1950 was about 2.4%. Again this must be considered in models. The ^{14}C produced by nuclear testing became measurable in 1954 (Broecker and Walton, 1959).

Our knowledge of the $^{14}C/C$ distribution within the sea is based on measurements on water samples taken at various regions and water depths and on measurements of $CaCO_3$ formed by marine organisms at known times in the past [historically dated shell collections (Broecker, 1963) and corals dated by ring counting (Druffel and Linick, 1978; Nozaki, Rye, Turekian, and Dodge, 1978)]. As only a limited number of water samples were collected prior to the onset of large-scale nuclear testing, the results of measurements on these samples are extremely important in distinguishing natural from bomb ^{14}C. For deep waters, measurements on post-1954 samples are adequate as significant amounts of bomb-produced ^{14}C have not as yet penetrated to great depth in the ocean (as demonstrated by the absence of measurable tritium in these waters).

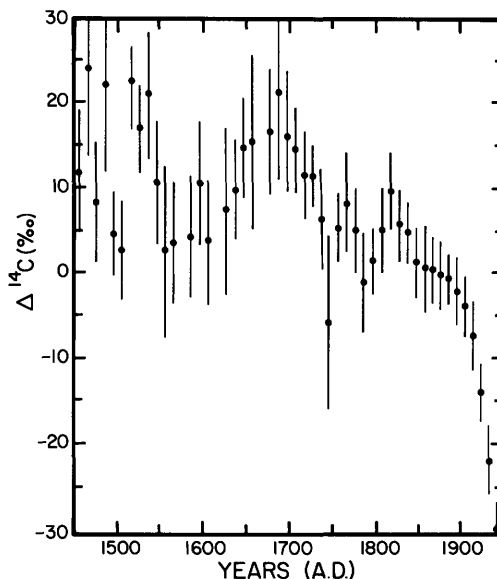As the counters used to measure radiocarbon cannot easily be absolutely calibrated, ^{14}C measurements are

Figure 15.2 $\Delta^{14}C$ for atmospheric CO_2 from 1450 to 1950 as reconstructed from tree ring measurements (Damon, Lerman, and Long, 1978). Prior to 1900 the variations must reflect changes in the production rate of natural ^{14}C. The decline subsequent to 1900 is caused by the release of ^{14}C-free CO_2 as the result of burning fossil fuels.

made by comparison with a standard (National Bureau of Standards oxalic acid). The results are given as per mil difference between the specific activity A of the sample carbon and 0.95 times the specific activity of a standard carbon sample (the 0.95 multiplier is chosen to bring the activity of the standard close to that of age-corrected 1850 wood; Broecker and Olsen, 1959, 1961).

In order to separate the ^{14}C differences produced by isotope fractionation, the $^{14}C/C$ ratios in the samples are normalized to a common $^{13}C/C$ ratio (Broecker and Olsen, 1959, 1961). The formulas used in these calculations are as follows:

$$\delta^{14}C = \frac{A_{samp} - 0.95 A_{NBS\ stan}}{A_{NBS\ stan}} \times 1000,$$

$$\Delta^{14}C = \delta^{14}C - (2\delta^{13}C + 50)\left(1 + \frac{\delta^{14}C}{1000}\right),$$

$$\delta^{13}C = 1000\frac{^{13}C/^{12}C)_{samp} - ^{13}C/^{12}C_{stan}}{^{13}C/^{12}C_{stan}}.$$

Table 15.3 gives the $\Delta^{14}C$ values for natural radiocarbon in a variety of water types. The range is about 200 per mil (from −40‰ for temperate surface water to −250‰ for 2500-m-depth water in the North Pacific). This distribution reflects not only the nite mixing rate of waters within the sea but also the finite rate of carbon-isotope equilibration between atmospheric CO_2 and surface ocean ΣCO_2. The difference between the ΣCO_2 content of average deep water and average surface water bears witness to the removal of carbon

Table 15.2 Distribution of Natural Radiocarbon among Reservoirs

	ΣC $(10^{16}$ moles)	$\frac{^{14}C/C}{(^{14}C/C)_{atm}}$	$\Sigma^{14}C$ $(10^4$ moles)
Atmosphere[a]	5	1.00	6
Ocean	280	0.87	290
Ocean sediments	—	—	~10[b]
Terrestrial biosphere	~7	0.95	~8
Soils	~20	0.90	~2
Continental sediments	—	—	<1

a. The absolute $^{14}C/C$ ratio for preindustrial atmospheric CO_2 was about 1.2×10^{-12}, corresponding to a specific activity of 8.0 dpm (gm C)$^{-1}$.
b. Assumes calcite-rich sediments cover 20% of sea floor, that the mean calcite accumulation rate in these areas is 1.5 gm cm^{-2} per 1000 years, and that the initial $^{14}C/C$ for this calcite is equal to that for atmospheric carbon.

Table 15.3 $\Delta^{14}C$ Values for Various Water Types in the Ocean

Water type	$\Delta^{14}C$ (‰)
Surface Waters	
Temperate	-40
Equatorial	-60
Deep Atlantic	
New LSW	-70
New GFZW	-70
New DSW	-70
NADW (mean) N. Western Basin	-100
NADW (mean) Eastern Basin	-115
AABW	-160
Deep Antarctic	
Circumpolar	-160
Deep Pacific	
Samoan Passage Overflow	-190
N. Pac. Bottom	-225
N. Pac. 2500 m	-250
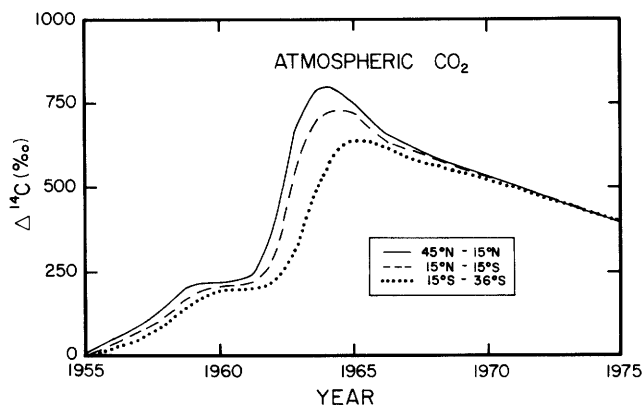
Figure 15.3 Excess atmospheric ^{14}C (resulting from bomb testing) as a function of time based on direct measurements of the $^{14}C/C$ ratio in tropospheric CO_2 samples. These measurements were made mainly by Nydal, Lövseth, and Gulliksen (1979). (See figure 16.1.)

from the photic zone by organisms and its return to dissolved form at depth in the sea. This "short crcuiting" by raining particulate debris must be taken into account in models used to derive ventilation rates from the $^{14}C/C$ distribution. This is done by joint consideration of the stable carbon and radiocarbon distributions (Lal, 1962, 1969; Craig, 1969; Broecker and Li, 1970).

Bomb-produced radiocarbon: Beginning with the first fusion-bomb tests in 1954 significant amounts of anthropogenic ^{14}C appeared in the atmosphere. The $^{14}C/C$ ratio in atmospheric CO_2, which had been falling since the turn of the century, began to rise sharply. This increase continued until 1963 when the U.S.-Soviet ban on atmospheric testing was implemented. Since then the atmospheric $^{14}C/C$ ratio has been steadily falling (see figure 15.3). This decrease reflects the dilution of the bomb-produced ^{14}C through mixing with ocean and terrestrial biosphere carbon.

Through gas exchange with the atmosphere the surface ocean has taken up bomb ^{14}C. Concurrent vertical mixing has carried this ^{14}C to the interior of the ocean. Profiles of total ^{14}C (natural plus bomb) as measured during the GEOSECS program are shown in figure 15.4. From the data we have concerning the prebomb distribution it is possible to estimate the depth distribution of the excess due to bomb testing. An ocean-wide mean penetration depth of about 300 m is obtained as of 1973 (the mid-point of the GEOSECS Atlantic and Pacific field programs).

As of 1973 the distribution of bomb ^{14}C was as follows. About 35% remained in the atmosphere, about 45% had entered the ocean, and about 20% had taken residence in the terrestrial biosphere (table 15.4). Within the oceans the bomb-produced ^{14}C is symmetrically distributed about the equator. The temperate gyres (15-45°) have considerably higher water-column inventories (i.e., bomb-produced ^{14}C atoms cm^{-2}) than does the equatorial belt (Broecker, Peng, and Stuiver, 1978). I shall discuss the oceanographic implications of this equatorial anomaly later in the paper.

Natural tritium: Like radiocarbon, tritium is produced by cosmic rays (von Buttlar and Libby, 1955). The production rate is estimated to be about 0.25 atoms cm^{-2} s^{-1} (Craig and Lal, 1961). It enters the ocean via vapor exchange and rainfall shortly after its birth in the atmosphere. As relatively few measurements of oceanic tritium were made before the commencement of nuclear testing, our knowledge of its distribution is rudimentary (Giletti, Bozan, and Kulp, 1958). Furthermore, because the blank corrections associated with these measurements were quite large and also quite uncertain, the validity of these data remains in question. Consequently, little use can be made of natural tritium in ocean-mixing studies. Fortunately the amount of this tritium is surely too small to be signif-
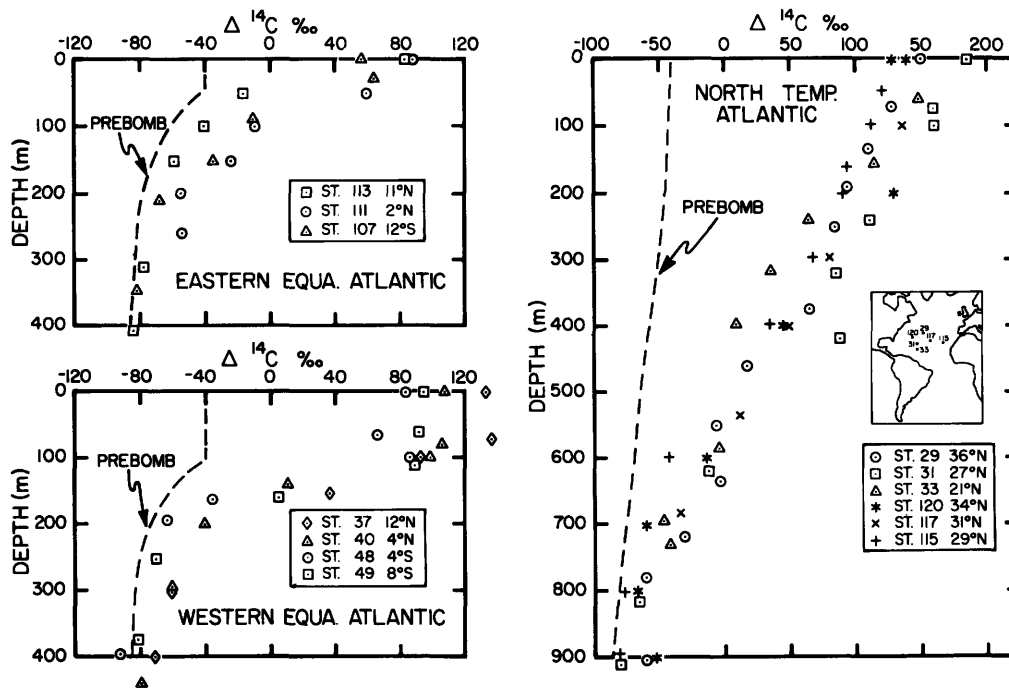
Figure 15.4 $\Delta^{14}C$ vs. depth in the north temperate and equatorial Atlantic Ocean as measured by Stuiver at the University of Washington and Östlund at the University of Miami on samples collected in 1972 as part of the GEOSECS program.

icant in modeling the distribution of tritium produced during nuclear testing.

Bomb-produced tritium: Nuclear tests during the 1950s and early 1960s produced large amounts of tritium (Begemann and Libby, 1957). As most of this production was during tests in the *northern* hemisphere, this tritium was added mainly to the northern-hemisphere stratosphere. From here it leaked to the troposphere (on a time scale of a year or so). Once in the troposphere it is removed to the land and ocean surface by vapor exchange and rainfall (on the time scale of weeks). Fortunately there are enough tritium data on rains and tropospheric water vapor collected during the peak fallout years to permit a reasonably sound reconstruction of the temporal and geographic pattern of its input to the ocean.

Furthermore, a picture of the time history for bomb tritium in at least the northern-hemisphere surface ocean can be reconstructed from measurements made between 1965 and the present.

Maps showing the tritium content of surface water are given in figure 15.5. As would be expected, the tritium content of northern-hemisphere surface waters is on the average much greater than that for southern-hemisphere surface waters. The boundary between these high- and low-tritium-content waters, however, lies near 15°N rather than at the equator. As discussed below, this unexpected result has important implications with regard to the dynamics of the equatorial thermocline.

Table 15.4 Distribution of Bomb ^{14}C as of 1974

|	Effective ΣC (10^{16} moles)	% Bomb ^{14}C
Atmosphere	5	~35
Surface ocean	~20[a]	~45
Terrestrial biosphere	~3[b]	~20

a. Assumes a characteristic penetration depth of 300 m and a bomb $^{14}C/C$ ratio for surface ocean water averaging 30% of that in the air (in 1973).
b. Assumes a characteristic replacement time of 15 years and the terrestrial biomass given in table 15.2.

441
Geochemical Tracers and Ocean Circulation
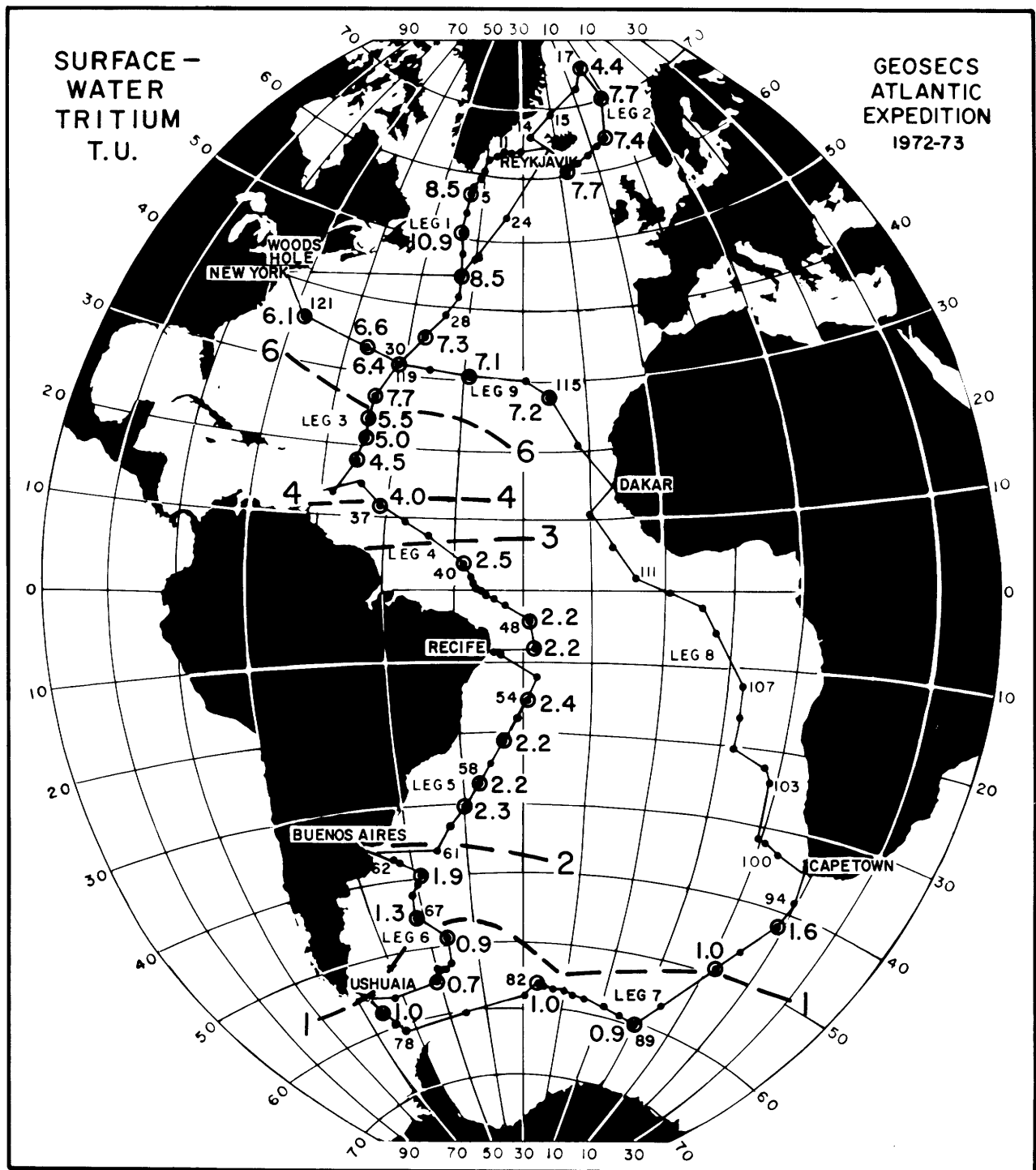
(15.5A)

Figure 15.5 Maps showing the geographical pattern of tritium concentrations in surface ocean water as determined by the GEOSECS program in the Atlantic (A) and Pacific (B) Oceans. The measurements were made by Östlund of the University of Miami. The units are T.U. (i.e., 10^{-18} T atoms per H atom).

SURFACE-WATER TRITIUM T.U.

GEOSECS PACIFIC EXPEDITION 1973-74
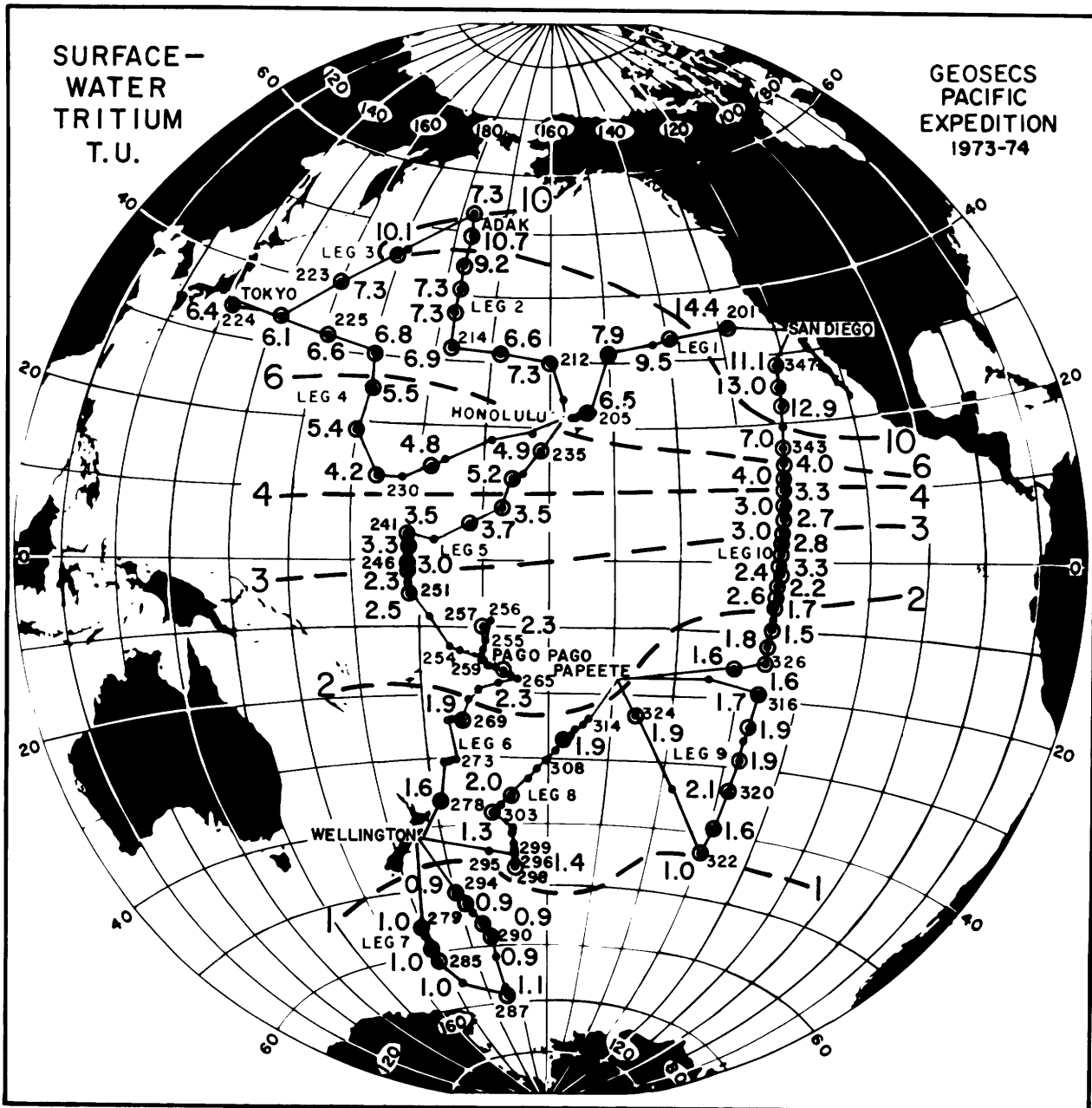
(15.5B)

Primordial ³He: Clarke, Beg, and Craig (1969) discovered that primordial ³He stored in the mantle is gradually leaking into the deep sea. Subsequent work has shown that this leakage is mainly from centers of sea-floor spreading in the Pacific Ocean. This ³He has been shown to diffuse laterally away from the ridge crest, forming a Pacific-wide "plume" centered at about 2500 m depth. This excess ³He can be distinguished from the atmospheric component either by subtracting the air-saturation value of ³He content from the observed ³He content or by comparing the ³He/⁴He ratio in the water sample with that in atmospheric helium (corrected by 1.4% for higher solubility of ⁴He relative to ³He). The ratio method is preferred because the abslute-concentration approach is made somewhat uncertain by the fact that deep-sea water appears to be several percentage points supersaturated with conservative atmospheric gases such as N_2, Ar, and Ne, and hence is probably supersaturated with He as well. This supersaturation is presumably induced by evaporative cooling of a surface film or by bubble entrainment generated by breaking waves. As measurements (Lupton and Craig, 1975) of sea-floor hydrothermal samples and of ridge-crest volcanic glasses reveal that the ³He/⁴He ratio in the exhaled mantle gas is rather uniform (eight to ten times larger than that in atmospheric helium), if the excess ³He is known to be solely of mantle origin (rather than in part from the decay of tritium), then the excess can be calculated from the ³He/⁴He ratio alone.

One of the interesting results of the measurements of excess ³He in deep water is the contrast between the Atlantic and Pacific (Lupton, 1976). The Pacific shows a large (up to 30%) mid-depth anomaly (figure 15.6). This anomaly has its origin in the East Pacific Rise. By contrast the excess ³He in the Atlantic is carried mainly by water returning from the Pacific via the Antarctic Bottom Water (Jenkins and Clarke, 1976). The anomalies generated by ³He release in the Atlantic are very small, the largest lying along the continental margin in the western North Atlantic rather than near the ridge crest (figure 15.7).

Radiogenic ³He: The decay product of ³H is ³He. In subsurface waters the ³He produced by the decay of ³H remains in the water (mass 3 is conserved). When waters containing radiogenic ³He reach the surface, however, the excess ³He escapes to the atmosphere. Hence the ratio ³He/³H in a subsurface water sample contains information with regard to its time of isolation from the surface (Jenkins and Clarke, 1976). Fortunately the ³He produced by the decay of tritium is spatially separated from that of the ³He leaking from the mantle. Where a significant overlap is suspected, the two excess components could be separated by precise measurements of absolute ⁴He concentration (coupled with Ne, Ar, and N_2 measurements aimed at es-
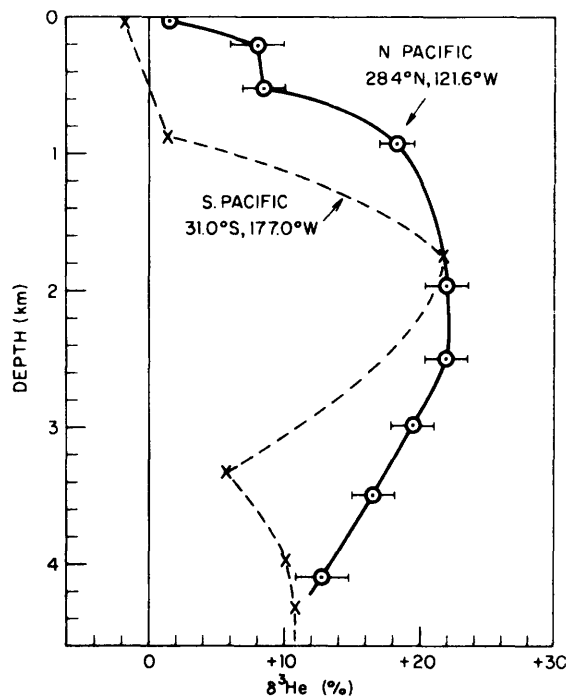

Figure 15.6 Distribution of excess ³He with depth in the Pacific. The profiles are by Clarke, Beg, and Craig (1970).

tablishing the degree of He supersaturation). The excess ⁴He content could then be multiplied by the ³He/⁴He ratio for average mantle-derived helium to yield the mantle component of the ³He excess. The residual ³He excess would then be that due to the decay of ³He. In practice this proves difficult because the ratio ³He/⁴He in mantle helium is an order of magnitude higher than that in atmospheric helium. A 1% error in the measurement of ⁴He concentration would lead to a δ³He error of about 10%.

²²⁶*Ra*: ²²⁶Ra is added to the ocean by diffusion from deep-sea sediments. With a half-life of 1600 years it has been a prime candidate for a mixing tracer (Pettersson, 1955; Koczy, 1958). Several factors have dimmed these hopes. First it was found that the deficiency of ²²⁶Ra in surface water relative to deep water is far too large to be explained by radiodecay. Removal of ²²⁶Ra on settling particulate matter was invoked to explain this difference. This hypothesis was confirmed by measurements of barium (Wolgemuth and Broecker, 1970). As barium and radium are nearly identical in their chemical behavior, it was hoped that through the use of ²²⁶Ra/Ba ratios (analogous to the use of ¹⁴C/C ratios) the effects of particulate transport could be separated from those of mixing [see Chan et al. (1976) for a discussion of the GEOSECS results].

This strategy suffers, however, from a severe problem of dynamic range (i.e., ratio of signal to observational error). If the deep sea is ventilated on a time scale of 1000 years, then for a tracer added mainly to the bot-

STATION NUMBER

(15.7A)

STATION NUMBER
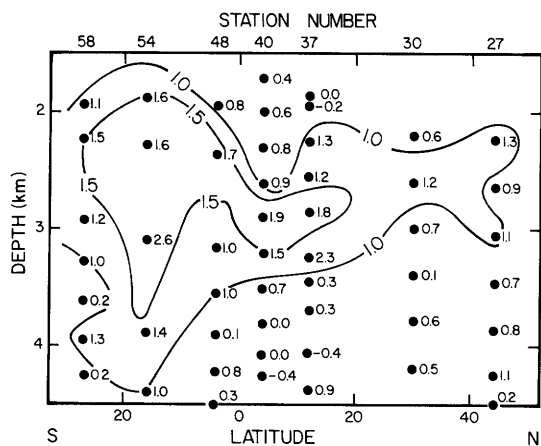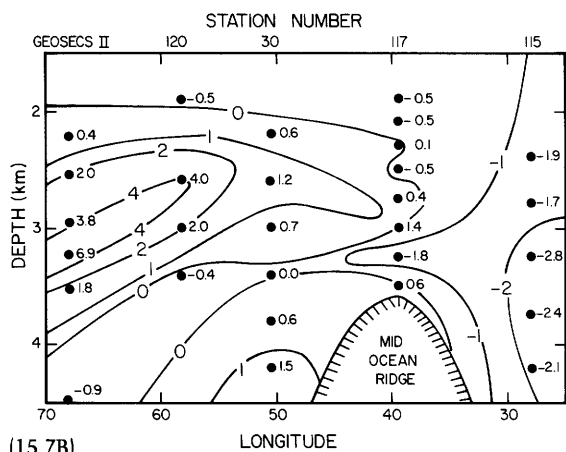
(15.7B)

Figure 15.7 Sections along the western Atlantic basins GEO-SECS track (A) and the GEOSECS track across the North Atlantic (B), showing the ^{3}He anomalies generated within the Atlantic Ocean (given in percentage of ^{3}He excess over atmospheric). The contribution of excess ^{3}He carried by deep waters returning to the Atlantic from the Pacific (via the Antarctic) has been eliminated through use of the linear "NO"-SiO$_2$ relation for deep Atlantic waters (see Broecker, in press). The data on which these plots are based are from Jenkins and Clarke (1976) and Lupton (1976).

tom of the sea the percentage difference Δ between the ratios of radioisotope to "carrier" ratio in deep water and in surface water should be approximately

$$\Delta = 100 \left\{ 1 - \exp \left[\frac{1000(VS/VD)}{\tau_{isotope}} \right] \right\} .$$

For a ratio of VS (volume of surface water) to VD (volume of deep water) of about 0.1, the surface-to-deep-water difference predicted for ^{226}Ra (half-life $\tau = 2300$ years) is only 6%. The observational error on the GEO-SECS ^{226}Ra measurements averages about 3% and that on a GEOSECS barium measurement about 1%. Thus any age message is buried in observational noise. Despite the fact that ^{14}C has a half-life 3.5 times *longer* than that of ^{226}Ra, because it enters the ocean from the top rather than from the bottom, it has a more than compensating advantage. As mentioned above, a 21% range is seen in the natural ^{14}C/C ratio within the sea. Thus the range of natural ^{14}C/C ratios in the sea should be about three times the range of ^{226}Ra/Ba ratios. Furthermore, the ^{14}C/C ratio can be measured with ten times higher precision ($\pm 0.4\%$) than the ^{226}Ra/Ba ratio ($\pm 4\%$). The overall dynamic-range advantage of ^{14}C over ^{226}Ra is thus thirty!

Although it may be possible to improve the measurement error for ^{226}Ra (to perhaps 1%), uncertainties in the geographical pattern of ^{226}Ra input from marine sediments will always plague the use of ^{226}Ra as a time tracer. For these reasons ^{226}Ra should perhaps be deleted from the list of mixing tracers. Nevertheless, as shown by results from the deep northeastern Pacific, where a great excess of ^{226}Ra relative to Ba has been found (Chung, 1976; Chung and Craig, in press), the ^{226}Ra distribution will contribute to our understanding of the release patterns of metals to deep water from sediments. Also, the ^{226}Ra distribution in the ocean must be known if we are to use the distributions of ^{228}Ra and of ^{222}Rn as time tracers for mixing, and if we are to use ^{210}Pb and ^{210}Po as time tracers for particulate processes.

^{228}Ra: ^{228}Ra has a half life of 5.8 years. Like ^{226}Ra it enters the ocean primarily by diffusion out of marine sediments (Moore, 1969). Because of its far shorter half-life, however, it has a much different distribution within the sea than does ^{226}Ra. Profiles with depth (see figure 15.8 for an example) show maxima at the surface and at the bottom with low values in the mid-water column. The high surface values reflect input of ^{228}Ra from the continental shelves coupled with rapid horizontal dispersion, and the high bottom values reflect the release of ^{228}Ra from deep-sea sediments. The low mid-depth values are the result of lower ratios of sediment area to water volume, and of the finite rate of vertical mixing. (The ^{228}Ra released from shelf and bottom sediments cannot reach this depth range before undergoing radiodecay.)
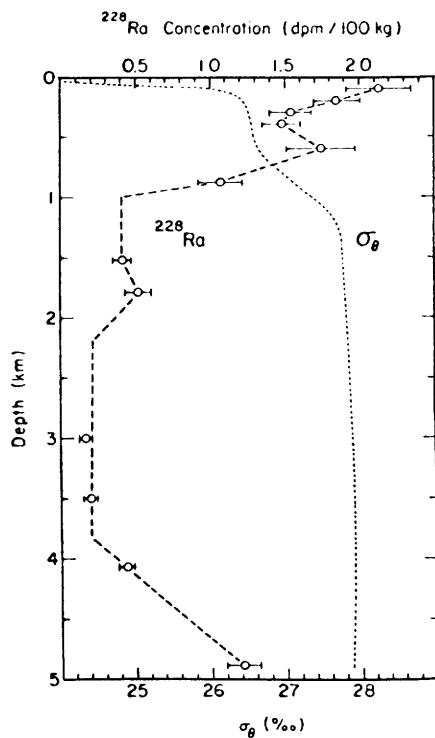
Figure 15.8 ^{228}Ra concentration as a function of depth at the GEOSECS Atlantic calibration station (36°N, 68°W) (Trier, Broecker, and Feely, 1972).

That ^{228}Ra that enters the deep sea probably can be treated as if it were chemically conservative. In surface water, however, removal by particulate matter may compete with radiodecay and mechanical mixing. For ^{226}Ra the probability of removal from surface water via particulate transport appears to be three times higher than by vertical mixing. If the residence time of water in the upper 400 m of the ocean is taken to be 50 years, then the residence time of ^{226}Ra with respect to particulate removal is about 18 years. As the mean life of ^{228}Ra is 8 years, correction for particulate transport effects may prove significant (i.e., ~20%).

^{222}Rn: Radon (half-life 3.85 days), is produced within the sea by the decay of ^{226}Ra dissolved in the sea. Well away from sedimentary margins of the ocean, in situ ^{226}Ra decay is the only source of ^{222}Rn. This is true for the surface mixed layer of the open ocean (the atmospheric ^{222}Rn content is too low to be a significant source). Loss to the atmosphere of the radon produced within the surface-ocean mixed layer provides a means of determining the rate of gas exchange between the ocean and atmosphere (Broecker, 1965). Close to the sediment-water interface, radon released from the upper few centimeters of the sediments (and from the upper few millimeters of Mn nodules and Mn-coated rock pavements) is found. This excess radon provides a means of determining the rate of mixing in the near-bottom ocean (Broecker, Cromwell, and Li, 1968). Both of these applications require a knowledge of the ^{226}Ra content of the water. To determine gas-exchange rates the difference between the equilibrium ^{222}Rn content (calculated from the ^{226}Ra content) and the observed mixed-layer ^{222}Rn must be known. For near-bottom mixing the sediment-derived ^{222}Rn is estimated by subtracting the ^{226}Ra-supported ^{222}Rn from the measured ^{222}Rn content of the abyssal water.

^{90}Sr and ^{137}Cs: The usefulness of fission products in oceanography was first demonstrated by Bowen and Sugihara (1957, 1958, 1960). Prior to nuclear testing the environment was free of the fission products ^{137}Cs and ^{90}Sr (both have half-lives close to 30 years). The amounts of these isotopes currently present in the ocean are entirely the result of these tests. Like ^{3}H they were added mainly to the northern-hemisphere stratosphere. Like ^{3}H they were deposited mainly in the northern hemisphere. Like ^{3}H their ocean distribution shows much higher water-column inventories north of 15°N than south of this boundary (Kupferman, Livingston, and Bowen, 1979). In fact they are so much like ^{3}H that no one has yet demonstrated that their oceanic distributions contain any information with regard to mixing not contained by the ^{3}H distribution (Dreisigacker and Roether, 1978). As ^{137}Cs and ^{90}Sr require far larger water samples than ^{3}H, as they cannot currently be measured with the accuracy or reliability of tritium, and as there are indications that ^{137}Cs may not be conservative within the sea, emphasis has been placed by most geochemists studying mixing processes on the measurement and interpretation of tritium data.

^{90}Sr should, however, not be written off as a mixing tracer. Its input distribution at the earth's surface is better known than that of ^{3}H (because it accumulates in soils). It has a longer half-life (30 years) than does ^{3}H (12 years), and therefore will be around for a longer time. Its concentration in tropical surface water has been recorded by corals (there is no similar paleotritium recorder).

^{85}Kr: ^{85}Kr is a product of fission. Thus it is produced during bomb testing, plutonium production, and power-reactor operation. Much of that produced has leaked to the air (Pannetier, 1968; Schroeder and Roether, 1975; Telegadas and Ferber, 1975). Measurements reveal a strong buildup in this reservoir (see figure 15.9). By gas exchange ^{85}Kr reaches the surface ocean (its current specific activity is about 3 dpm m^{-3}). Because of this very low activity only a few measurements of ^{85}Kr have been made in the sea to date (Schroeder, 1975). As expected, its vertical distribution shows a first-order similarity to that of the other anthropogenic tracers (^{3}H, ^{14}C, ^{90}Sr, ^{137}Cs). If this covariance were perfect, then there would be no interest in
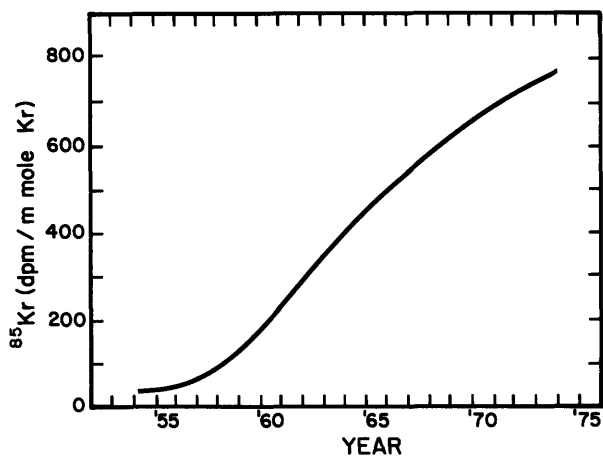
W. S. Broecker

Figure 15.9 ^{85}Kr as a function of time in the atmosphere (Schroeder and Roether, 1975).

going to the trouble to collect and process the large water samples necessary for measuring this isotope.

There is, however, at least one very important application for this isotope. As is discussed at greater length later in the paper, a difficulty arises in estimating the concentration of excess CO_2 (i.e., that stemming from the production of fossil fuels) in currently forming deep water. Because the chemical equilibration time of CO_2 between mixed-layer water and the atmosphere is of the order 1 year while the cooling time is on the order of 1 month, newly formed deep waters are likely to carry less than their capacity of excess CO_2. The most promising approach to finding how much less appears to be through the use of two tracer gases: one a gas that equilibrates on a time scale longer than that for CO_2, and the other a gas that equilibrates on a time scale shorter than that for CO_2. $^{14}CO_2$ is the only choice for the former. As discussed by Broecker, Peng, and Takahashi (in press) the isotopic equilibration time for carbon exceeds the chemical equilibration time by a value numerically equal to the buffer factor (~12 for cold surface water). ^{85}Kr and the freons are the prime candidates for the short-exchange-time gas. Like all gases of normal solubility their exchange time is about 1 month (Peng et al., 1979). Although the freons have the advantage that inexpensive measurements can be made on small samples, they have yet to be proven conservative in sea water. Proof of their long-term stability can only be achieved through comparison with a second tracer of the same type. ^{85}Kr is the only candidate for this task.

^{39}Ar: Cosmic-ray-produced ^{39}Ar is the ideal deep-ocean tracer. As it exchanges rapidly with the air, the problem of establishing its concentration in newly formed deep water is far smaller than for ^{14}C. Its half-life of 270 years is far more appropriate to deep-water movement times than that of ^{14}C. The problem in its use is technical (Loosli and Oeschger, 1968, 1979; Oeschger et al., 1974). Very large samples (several tons) and ultralow background counting are needed. Only Loosli and his colleagues at the Bern laboratory currently are capable of measuring this isotope in the sea. Because its potential is so large, however, the next decade is bound to bring forth many ^{39}Ar measurements.

^{32}Si: Since Schink's (1962) early attempts, two decades of effort have gone into determining the distribution of ^{32}Si (a cosmic-ray-produced isotope with a half-life of ~250 years) in the sea. Like ^{39}Ar its collection and measurement are fraught with technical difficulties. Using the *in situ* extraction technique of Krishnaswami et al. (1972) about 200 samples were collected during the GEOSECS program. Three profiles have been published (Somayajulu, Lal, and Craig, 1973). The remainder of the analyses are still in progress at the Physics Research Laboratory at Amedabad in India. Even when these data appear, three serious problems will remain for their interpretation. First, the performance of the bag samplers used to collect the silica was far from perfect. Second, since the particulate cycle dominates the movement of silica down the water column, isolation of the water dynamics from the particle dynamics constitutes a difficult problem. Finally, the measurement errors are sizeable and will surely lead to considerable ambiguity in the interpretation. If the ^{39}Ar method succeeds, ^{32}Si may well be relegated to the area of particulate research. Were the circulation dynamics independently known, the ^{32}Si distribution could tell us much about the pattern of dissolution of siliceous particles.

Freons: Most of the freon produced as a propellent and as a refrigerant ultimately finds its way to the atmosphere. Reliable and accurate means of measuring it in air and sea water have been worked out (Lovelock, Maggs, and Wade, 1973). Measurements on sea water show its distribution to be similar to that of tritium and other "fallout" nuclides (Hahne et al., 1978). As mentioned above, once it can be established that freons are conservative in the sea, then this substance will become one of the more useful of the transient tracers.

^7Be: With a half life of 53 days, cosmic-ray-produced ^{7}Be has great potential as a tracer of upper thermocline processes (Silker, 1972a,b; Silker et al., 1968). An example of its distribution in the upper water column is shown in figure 15.10 (36°N, 68°W). Unfortunately, because of the large volume of water needed (thousands of liters) and of the complexity of the counting system needed for its detection, little work has been done to take advantage of the information carried by this isotope. Were it to be used, attention would have to be given to its removal by particulate matter and to the seasonal variation in its distribution.
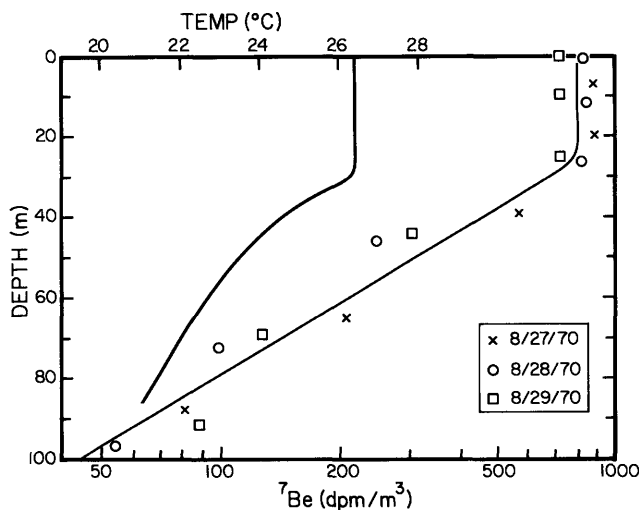
Figure 15.10 ^{7}Be as a function of depth at the GEOSECS Atlantic calibration station (36°N, 68°W) occupied during August 1970 (Silker, 1972a). Solid curve is temperature profile.

15.3 Water-Mass Tracers

All deep waters in the ocean are mixtures from two or more sources. Since the concentrations of the time tracers in each source are potentially different, these mixtures must be unscrambled if we are to use the isotope data successfully to yield ventilation rates. For this job we need properties that are conserved once the water ends contact with the atmosphere. Candidates are as follows:

(1) Conductivity. The conductivity of a water parcel isolated in the deep sea changes only because small amounts of SiO_2, CO_2, PO_4^{---}, Ca^{++} and NO_3^- are added via respiration and mineral solution. As discussed by Brewer and Bradshaw (1975), these changes are just measurable. For any of the applications involving radioisotope "dating" of sea water, the salinities calculated from conductivity measurements may be treated as perfectly conserved.

(2) Temperature. As heat transfer by molecular conduction is of negligible importance to the internal energy content of a sea water parcel, potential temperature can be treated as conservative. The only *source* of heat within the deep sea of significance is geothermal heat. Except in rare circumstances this contribution is small enough not to create difficulties. Because heat-flow rates are well known (except perhaps along ridge crests), the effects of geothermal heating can often be taken into account in models of radioisotope data (i.e., the temperatures can be corrected by iteration).

(3) ^{2}H and ^{18}O. The isotopic composition of the waters ventilating the deep sea varies from source region to source region (Epstein and Mayeda, 1953). As discussed by Craig and Gordon (1965), these variations do not strongly correlate with either salinity or temperature.

The isotopic messages from ^{2}H and ^{18}O, however, are highly correlated with each other. These signatures are conservative. The problem lies with the measurements. An acceptable dynamic range can be achieved only by painstaking care using the best available mass spectrometers and preparation lines. Because of this only a limited number of such measurements is currently available. Even for measurements of the highest attainable precision the dynamic range may prove to be too small to be useful.

(4) "NO" and "PO". Although dissolved-oxygen gas is utilized by animals and bacteria living beneath the photic zone in the sea, a correction can be made for this utilization by taking into account the fact that for each 135 molecules of O_2 consumed about 15 molecules of NO_3^- and about one molecule of PO_4^{---} are released to the water as dissolved ions. Thus the sums $[O_2] + 9[NO_3]$ and $[O_2] + 135[PO_4]$ are potentially conservative properties (Broecker, 1974). The near constancy of the NO_3/PO_4 ratio in most parts of the deep sea supports this concept. Since the coefficients 9 and 135 are not truly "stoichiometric" quantities, however, care must be taken in using "NO" and "PO". The actual coefficient applying to any given mass of water might deviate from these values. "NO" has an additional drawback. In areas of the ocean where the dissolved O_2 content reaches 1% or less of its saturation value, NO_3 is used by bacteria as an oxidant. Thus, in regions adjacent to zones of severe O_2 depletion (like the thermocline off Central and South America), "PO" rather than "NO" should be used in "unmixing" calculations.

(5) SiO_2 and Ba. Silica and barium are concentrated in deep waters relative to surface waters, and show large differences from water type to water type (Edmond, 1974; Chan, Drummond, Edmond, and Grant, 1977; Chung and Craig, in press). As these differences are generated by the removal of these substances from the upper ocean followed by regeneration in the deep ocean, Ba and SiO_2 are by no means conservative. Nevertheless, observation has shown that in certain regions of the ocean they are nearly conservative and can be successfully used for "unmixing" calculations. An example is given below.

15.4 Modeling Tracer Data

The ultimate use of the radioisotope data is to obtain information regarding transport of water and of species dissolved in the water within the sea. Deconvolution of the tracer field into the various modes and directions of transport remains an unsolved problem. As might be expected, modeling of radioisotope data has undergone an evolution that paralleled the size and quality of the data set. The first models were of the box variety.

The ocean-atmosphere system was approximated by a few well-mixed reservoirs. The ^{14}C data were used to define transfer coefficients between these reservoirs. Initially, three-box models that separated the system into a well-mixed atmosphere, a well-mixed surface ocean, and a well-mixed deep ocean were used (Craig, 1957). The fluxes derived were the air-sea gas exchange rate and the water transfer rate across the main thermocline. When ^{14}C data for the Pacific Ocean (Bien, Rakestraw, and Suess, 1963) as well as the Atlantic Ocean (Broecker, Gerard, Ewing, and Heezen, 1960) became available, a large difference in the apparent age for the deep water in the two oceans became evident. This generated an incentive for models with more boxes. It was also realized that the regions of deep-water formation (North Atlantic and Antarctic) should be treated separately. Various attempts were made to generate multibox models (Broecker, 1963; Keeling and Bolin, 1967, 1968; Broecker and Li, 1970). In all these attempts, owever, it was realized that because the number of fluxes needing definition increased as the square of the number of boxes while the number of new pieces of information increased linearly with the number of boxes, this approach was destined to yield a considerable degree of ambiguity. The idea of using salinity and temperature to aid in the definition of fluxes, while promising in a mathematical sense, also proved impractical because of the uncertainties in the atmospheric boundary conditions for heat and salt. Geochemists fell back to the use of the simpler three-box models as a guide to geochemical thinking, and suspended attempts to use box models to answer physical oceanographic questions.

Munk (1966) initiated an alternate approach to the use of isotope data. He focused his attention on the trend of $^{14}C/C$ ratio with depth within the deep Pacific and showed that, if the type of advection-diffusion model used by Stommel (1958), Robinson and Stommel (1959), Stommel and Arons (1960b) and Wyrtki (1961b, 1962) were employed, the ^{14}C trend would yield absolute values for the upwelling velocity and the vertical diffusivity. Craig (1969) elaborated on Munk's idea, pointing out that ^{14}C and C should be treated separately in the calculation. By fitting both the ^{14}C concentration profile and the ΣCO_2 concentration profile, the contribution of ^{14}C through the rain of particulates could be accounted for. A reader interested in a review of this subject is referred to the excellent paper by Veronis (1977). As the GEOSECS data came in, it became apparent that the horizontal gradients within the deep Pacific could not be neglected. For this reason interest in the simple one-dimensional advection-diffusion has waned.

Kuo and Veronis (1970, 1973) initiated the first two-dimensional modeling of the deep-ocean tracer field including advection and diffusion. They assumed that deep water formed at two small high-latitude regions and upwelled uniformly over the entire ocean. They used a modified form of the horizontal advection pattern envisioned by Stommel (1958), and assumed uniform lateral and vertical diffusion rates. Their endeavors focused on matching the deep-O_2 distribution. Fiadeiro and Craig (1978) adopted a variation on this approach and did more elaborate three-dimensional calculations for the deep Pacific. Interest in this approach has also waned, however, because of serious reservations with regard to the suitability of the advection pattern adopted for the models.

During the last 2 years Sarmiento has been applying fluxes of bomb-produced isotopes to Bryan's quasi-diagnostic model (Sarmiento and Bryan, in preparation), the idea being to see whether the model reproduces the observed distribution of these tracers. This work is still in progress.

Despite the failure to produce a satisfactory model with which to match the tracer data for purposes of elucidating the dynamics of deep-ocean ventilation, one very important application has emerged. Through tracer-tracer analog modeling the distributions of the radioisotopes can be used to predict how much fossil fuel CO_2 has been (and will be) taken up by the sea. A number of investigators have used three-box models calibrated using the distribution of natural radiocarbon (Bolin and Eriksson, 1959; Broecker, Li, and Peng, 1971; Machta, 1972; Keeling, 1973). Oeschger, Siegenthaler, Schotterer, and Gugelmann (1975) have used a vertical-diffusion model calibrated with natural radiocarbon. Broecker, Takahashi, Simpson, and Peng (1979) have subsequently shown that the diffusivity chosen by Oeschger et al. (1975) is consistent with the vertical distribution of the bomb-produced tracers. Several groups of investigators are currently developing more elaborate models of this type. While not giving us any better idea of the physics of ocean circulation, these models do provide us with an interim approach to a problem of great import to society.

15.5 Current Applications

We shall consider four applications of the tracer results. The first is the ventilation time of the deep sea. The single great triumph of the natural radiocarbon measurements in the ocean has been the establishment of a 1000-year time scale for the residence of water in the deep sea. Now that we have the GEOSECS data, what more can be said on this subject? The second is the ventilation time for the main oceanic thermocline. The transient tracers ^{14}C and ^3H prove ideal for this task. The third is the dynamics of deep-water formation. In this process the interaction between surface water and the atmosphere constitutes a rate-limiting step for the

tracers used. Again, the transient tracers prove ideal for the task. Finally, the distributions of the short-lived natural tracers and of the anthropogenic tracers allow *upper* limits to be placed on the rates of vertical (diapycnal) mixing.

15.6 Ventilation of the Deep Sea

Although a number of estimates of the mean ventilation time for the deep sea have been proposed, that of about 1400 years, based on radiocarbon, is the most widely quoted. In the three-box model the ventilation time T of the deep sea is given by the following equation:

$$T = \frac{V_D}{R} = \left[\frac{(^{14}C/C)_S}{(^{14}C/C)_D} - 1\right] T_{^{14}C},$$

where V_D is the volume of the deep sea, R the ventilation rate of the deep sea, $(^{14}C/C)_S$ and $(^{14}C/C)_D$ the carbon isotope ratios for the mean surface and mean deep ocean (prior to the industrial revolution), and $T_{^{14}C}$ the mean life of ^{14}C (i.e., 8200 years). Taking $(^{14}C/C)_S/(^{14}C/C)_D$ to be 1.17 ± 0.03 (i.e., $\Delta^{14}C_S = -50 \pm 10‰$ and $\Delta^{14}C_D = -190 \pm 20‰$), a ventilation time of 1400 ± 250 years is obtained. Among other things this model assumes that the ventilation times for water and carbon are equal. Because the $^{14}C/C$ ratio in newly formed deep water has been shown not to reach that observed for the warm surface ocean, the ventilation time for water is surely less than that given by the box model. If the box model calculations used to obtain this result were repeated using average $^{14}C/C$ ratios obtained from the GEOSECS data set, the result would not change significantly. Evolution in geochemical and oceanographic thinking since the heyday of box modeling makes clearer the problems associated with using ^{14}C data to estimate water residence times in the deep sea. Until means of overcoming these problems are achieved it will not be possible to evaluate properly the ventilation times derived from ^{14}C data, nor will it be possible to improve on them.

One problem is related to the fact that while the mixed layer of the ocean can be cooled (through contact with winter air) in a few weeks, equilibration between the $^{14}C/C$ ratio in the carbon dissolved in the mixed layer and that in the atmospheric CO_2 requires a decade or more. Harmon Craig recognized this problem long ago but until recently it has received only casual attention. The upshot is that the ^{14}C residence time in the deep sea must exceed the water residence time. Results from the Weddell Sea (Weiss, Östlund, and Craig, 1979) dramatically illustrate this point, for the new deep water formed there contains nearly the same $^{14}C/C$ ratio as ambient circumpolar deep water.

The other problem has to do with the recirculation of old water within the deep sea. Rarely is it possible to isolate the component of $^{14}C/C$ change due to *in situ* aging. Rather, the changes in $^{14}C/C$ ratio within a given deep-sea basin can be accounted for largely by the mixing of end members with different $^{14}C/C$ ratios. This greatly complicates the use of ^{14}C data to obtain the flux of deep water into a given basin.

The trend of $\Delta^{14}C$ along the 4000-m horizon is shown in figure 15.11. The pattern shows a gradual decrease in $^{14}C/C$ "down" the Atlantic and "up" the Pacific (with similar values in the Antarctic segments of the two oceans). The down-Atlantic decrease is about 80‰ and the up-Pacific decrease is about 70‰. While this might be interpreted as evidence for gradual aging as the water moves by advection slowly around the globe, a close look at the situation reveals that at least in the Atlantic the trend is largely the result of mixing between low $^{14}C/C$ waters of circumpolar origin and high $^{14}C/C$ waters of northern Atlantic origin. When this mixing is taken into account the residence time of water in the Atlantic is considerably decreased and the flux of new North Atlantic deep water necessary to maintain it is correspondingly increased (table 15.5).

Table 15.5 Evolution of Calculations of the Apparent ^{14}C Age of a NADW Sample with a $\Delta^{14}C$ of $-105‰$

	$\Delta^{14}C$ values					
	Warm surface water	New no. comp. water	New AABW	Δ due to mixing with AABW	Δ due to *in situ* aging	Apparent[a] age
Broecker et al. 1960	-28	(-28)	-155	0	-77	675
Broecker and Li 1970	-40	(-40)	-155	-12	-53	470
Stuiver (GEOSECS) 1976	—	-70	-160	-10	-25	225
Broecker (GEOSECS) 1979	—	-70	-160	-26	-9	80

a. $t = 8200 \ln \dfrac{1 - (\Delta^{14}C_{Initial}) \times 10^{-3}}{1 - (\Delta^{14}C_{Initial} + \Delta_{aging}) \times 10^{-3}}$.

W. S. Broecker
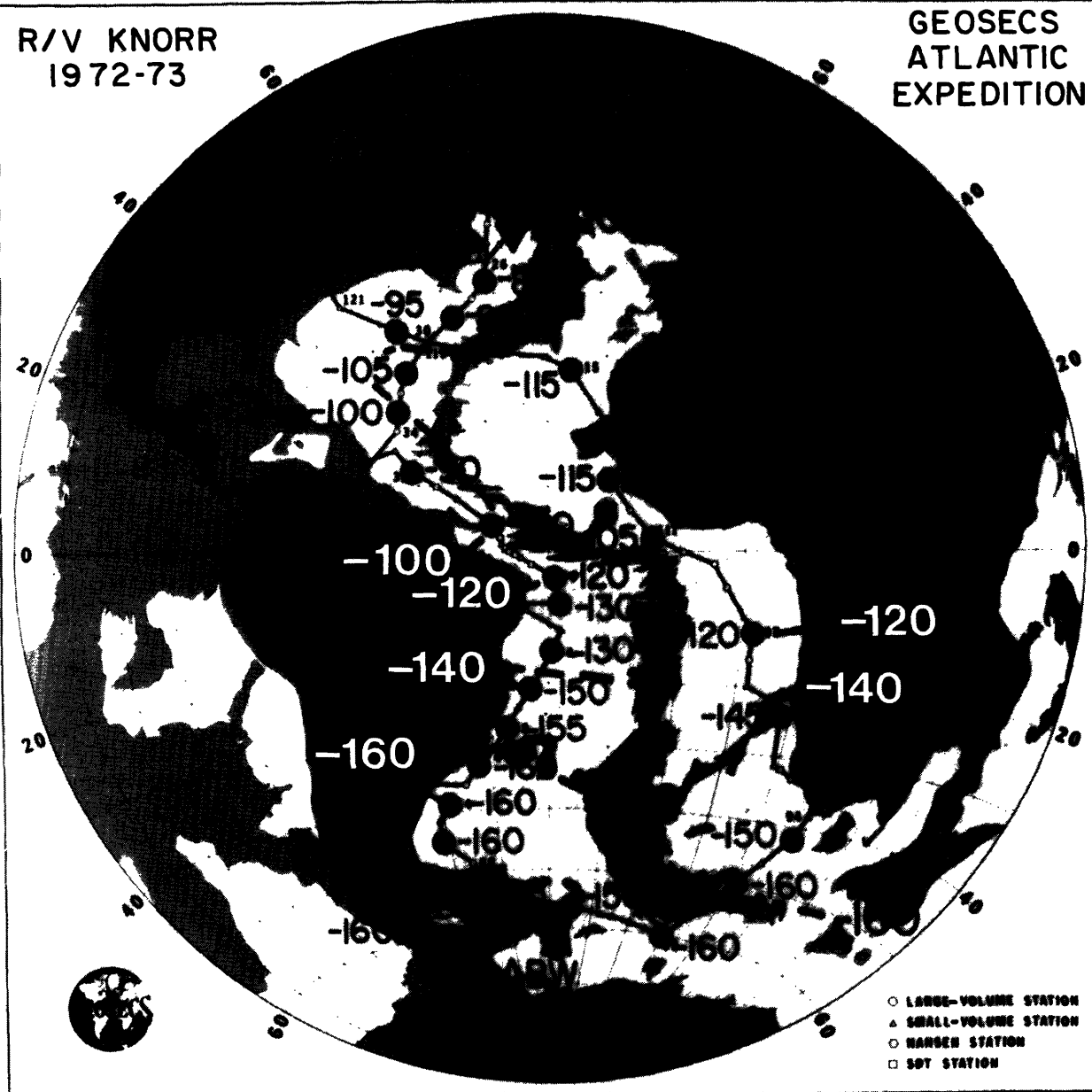
Figure 15.11 Maps showing the distribution of ^{14}C along the 4000-m horizon in the Atlantic (A) and Pacific (B) Oceans. The analyses were made by Östlund at the University of Miami and Stuiver at the University of Washington as part of the GEOSECS program.

R/V MELVILLE 1973-74

GEOSECS PACIFIC EXPEDITION

LARGE-VOLUME STATION
SMALL-VOLUME STATION
SDT STATION

(15.11B)

W. S. Broecker
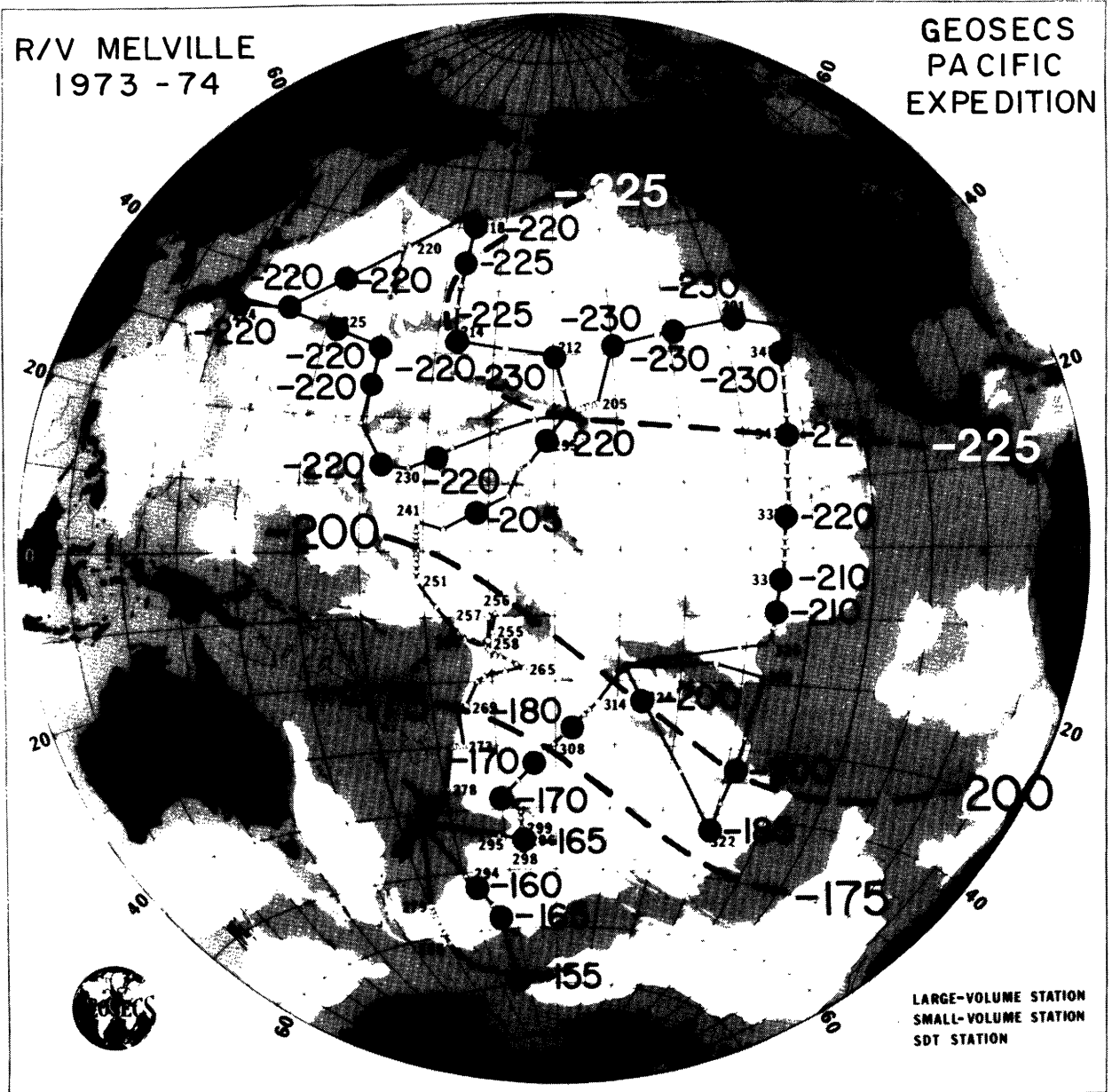
Before going into this matter further, it is appropriate to review the evidence leading to the conclusion that the back mixing of Antarctic deep water is the major cause for the $^{14}C/C$ gradient observed in the Atlantic. Confusion on this point has arisen because of the ambiguity in estimates based on conventional temperature-salinity (θ-S) analysis of the fractions of various contributing water types. There are three such northern water types: deep water formed by winter cooling in the Labrador Sea (LSW); water spilling over the sill connecting Iceland to Greenland (DSW); and water which ultimately comes from overflow across the sill connecting Iceland with the British Isles but enters the western basin through the Gibbs Fracture Zone. As shown in table 15.6, the traditional θ-S approach is not particularly sensitive, because the θ and S ranges for the three contributing northern water types are large compared to the differences from the dominant southern type, i.e., the Antarctic Bottom Water (AABW). Temperature and salinity could be used only if the relative proportions of the northern-source waters one to another were known. They are not (see chapters 1 and 2).

By contrast the SiO_2 and the "NO" contents of the three northern water types are almost identical and are very different from that for AABW (see figure 15.12). Thus, were either of these properties conservative, we would have a means of determining the fractions of high-^{14}C northern and low-^{14}C southern waters in any given sample from within the mixing zone. One test of conservation is a plot of SiO_2 versus "NO". Linearity would require either conservation of both properties or a fortuitous correlation between the true "NO" coefficient and the amount of SiO_2 added to any given sample through the dissolution particles. As shown in figure 15.12 the relationship is remarkably linear except for waters in the southern eastern basin.

If this linearity is (as I believe it can convincingly be shown to be) a demonstration of near conservancy of "NO" and SiO_2, then the fraction of southern component in each sample of deep Atlantic water collected by the GEOSECS program can be determined either from its SiO_2 or "NO" content (these two independent estimates generally agree to ±0.03). The plot of $\Delta^{14}C$ versus fraction of southern component so obtained is given in figure 15.13. The dominance of mixing is clearly demonstrated. The deviation attributable to radiodecay averages only 9‰ (the measurement error on a given sample averages 4‰).

The geographic and depth patterns of the residual anomalies (i.e., those produced by radiodecay within the Atlantic) are shown in figure 15.14. The only pronounced feature is the larger anomaly for the eastern than for the western basin. As shown in table 15.5, estimates of the residence time of waters in the deep western Atlantic have dramatically decreased with time. Part of this decrease is accounted for by the realization that water descending in the deep northern Atlantic has a lower $^{14}C/C$ ratio than ambient Atlantic surface water. The rest is due to the increase in the estimates for the role of AABW back mixing.

As I have shown in a separate publication (Broecker, 1979), if an advective model is used to reproduce both the distribution of northern and southern components in the western Atlantic and the distribution of the residual (i.e., in situ decay) anomalies, then a flux of 20×10^6 m^3 s^{-1} of northern component (some mixture of LSW, GFZW and DSW) and 10×10^6 m^3 s^{-1} of southern component (AABW) are needed. As the deep portions of the eastern basin are known to be ventilated from the western basin (via fracture zones), no extra flux of northern component water is needed for its ventilation (part of the water exiting the western basin does so through the Romanche and possibly other frac-

Table 15.6 Characteristics of the Contributors of the NADW Complex

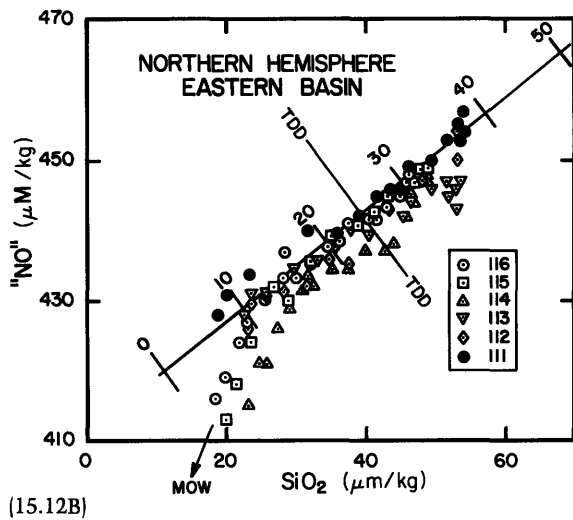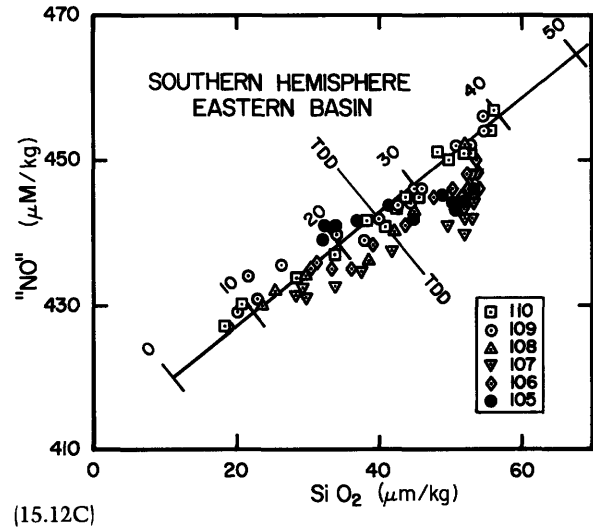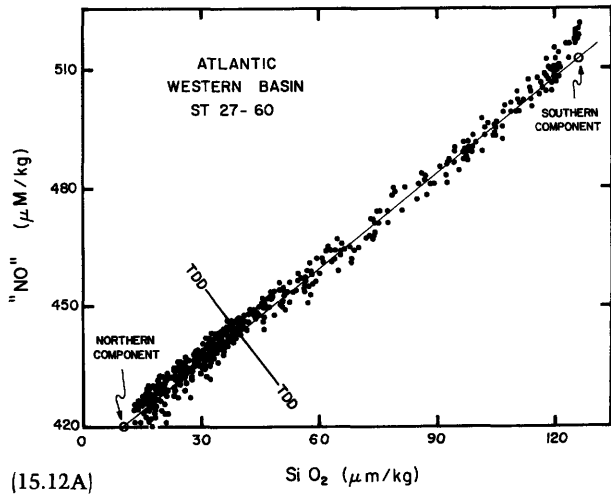| Water type	θ (°C)	S (‰)	"NO" (μM kg^{-1})	SiO_2 (μM kg^{-1})	$\Delta^{14}C$ (‰)
Labrador Sea Deep Water	3.3	34.94	430	12	−69
Denmark Straits Overflow Water	1.5	34.91	427	10	−69
Gibbs Fracture Zone Water	2.8	35.00	429	13	−63
Mediterranean Sea Overflow Water	12	36.4	300	8	~−60
Circumpolar Bottom Water	0.0	34.70	511	125	−163
Circumpolar Intermediate Water	2.2	34.63	472	85	−147

(15.12A)

(15.12C)

(15.12B)

Figure 15.12 Plots of "NO" versus SiO₂ for all the samples taken by the GEOSECS program below 1500 m in the Atlantic Ocean. In the western basin (A) the entire range of compositions between northern (DSW, LSW, and GFZW) and southern (AABW) component water is seen consistent with the two-end-member hypothesis. No change in slope is seen at the Two Degree Discontinuity (Broecker, Takahashi, and Li, 1976). In the northeastern basin (B) those stations nearest to the Straits of Gibraltar show a deviation toward low "NO" value for any given SiO₂ content caused by the admixing of low "NO" Mediterranean water (see table 15.6). Deep waters in the southeastern basin (C) show a deviation toward high silica at any given "NO" value. This presumably reflects *in situ* production of silica through the dissolution of particulate matter.
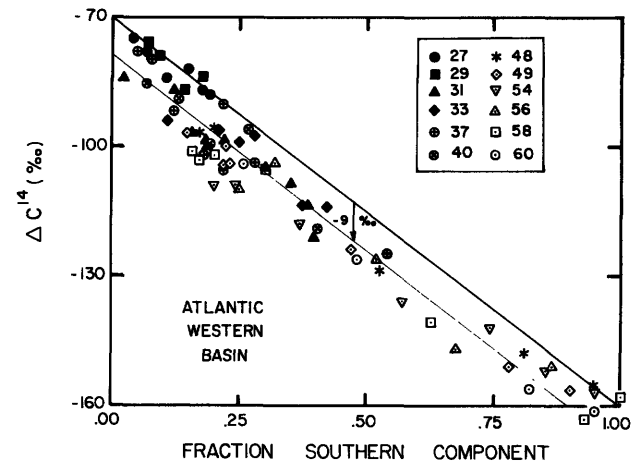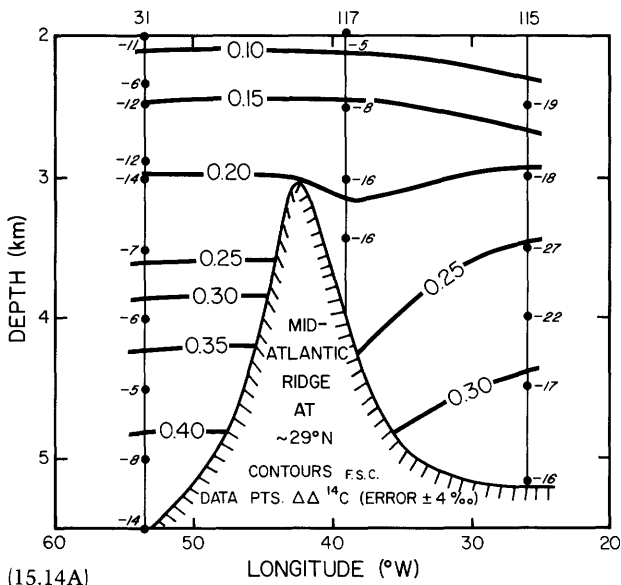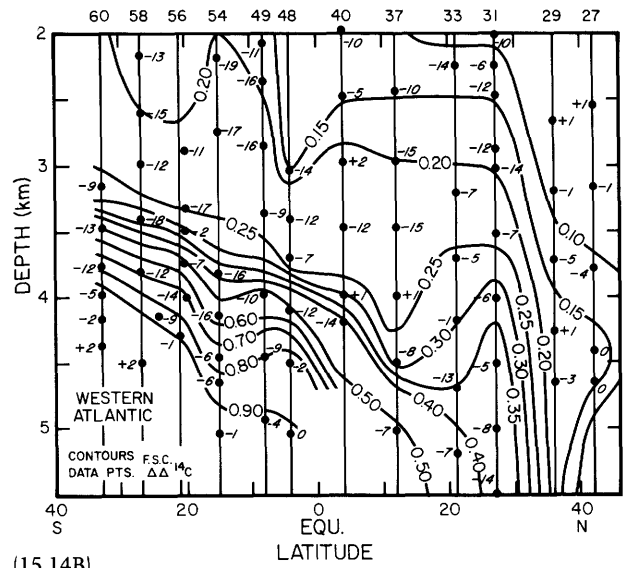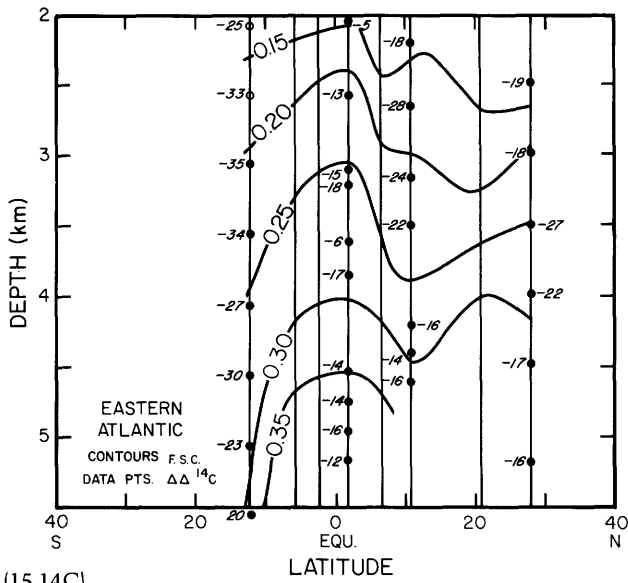

Figure 15.13 $\Delta^{14}C$ for western basin deep waters as a function of the fraction of southern component (F.S.C., as estimated from the "NO"-SiO₂ relationship). Were mixing alone responsible for the trend, then the points should lie along the line joining $\Delta^{14}C = -160‰$, F.S.C. = 1.0, and $\Delta^{14}C = -70‰$, F.S.C. = 0.0. Deviations below this line are presumably a measure of the loss of radiocarbon within the mixing zone by radioactive decay. The radiocarbon measurements were made by Stuiver of the University of Washington and Östlund of the University of Miami.
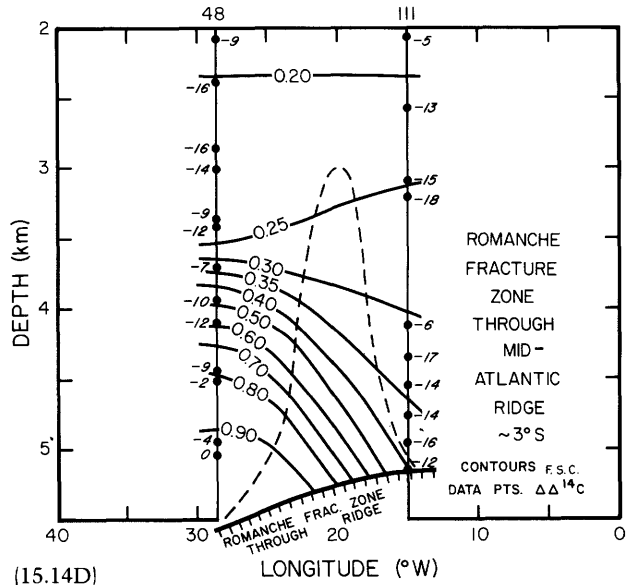
(15.14A)

LONGITUDE (°W)

DEPTH (km)

MID-ATLANTIC RIDGE AT ~29°N

CONTOURS F.S.C.
DATA PTS. ΔΔ ^{14}C (ERROR ± 4 ‰)

(15.14B)

WESTERN ATLANTIC

CONTOURS F.S.C.
DATA PTS. ΔΔ ^{14}C

LATITUDE

DEPTH (km)

(15.14C)

EASTERN ATLANTIC

CONTOURS F.S.C.
DATA PTS. ΔΔ ^{14}C

LATITUDE

DEPTH (km)

(15.14D)

ROMANCHE FRACTURE ZONE THROUGH MID-ATLANTIC RIDGE ~3°S

CONTOURS F.S.C.
DATA PTS. ΔΔ ^{14}C

ROMANCHE FRAC. ZONE THROUGH RIDGE

LONGITUDE (°W)

DEPTH (km)

Figure 15.14 Four sections showing the geographic and depth distribution of the ^{14}C anomalies attributable to radioactive decay within the deep Atlantic. The contours show the fraction of southern component (i.e., AABW) within the deep Atlantic.

455
Geochemical Tracers and Ocean Circulation

ture zones which cut the Mid-Atlantic Ridge). The question how much more water is needed to ventilate the eastern basin above the ridge crest is not so easily answered. I guessed that 10×10^6 m³ s⁻¹ more of northern component is required. If so, then the total flux of northern component is 30×10^6 m³ s⁻¹.

The volume of the deep sea (below 1500 m) divided by 30×10^6 m³ s⁻¹ gives 900 years. Thus, were North Atlantic Deep Water the only source of *carbon* isotope ventilation, the mean age of deep-sea carbon with respect to that entering with new deep water formed in the northern Atlantic would be *900* years. Starting with $\Delta^{14}C$ values of $-70‰$, this would give a mean $\Delta^{14}C$ for deep-sea carbon of $-167‰$ (a value close to the observed mean).

This does *not* imply that ventilation of the deep sea by waters descending around the continent of Antarctica is negligible. Rather, as shown by Weiss et al. (1979), these waters exhaust heat without substantially changing their ^{14}C value. Thus if, as commonly estimated, the flux of new deep waters formed around the perimeter of Antarctic is in the range 10 to 40 × 10⁶ m³ s⁻¹ (Gordon, 1975b; Gill, 1973; Killworth, 1974, 1977; Carmack, 1977), then the water ventilation time of the deep sea is probably considerably less than 900 years.

While these calculations are preliminary and subject to many criticisms, they do serve to indicate that derivation of water fluxes from ^{14}C data is far from a straightforward exercise. The conventional ^{14}C-residence time (based on box models) provides only an upper limit on the water-residence time. As temperature is probably the property most rapidly equilibrated with the atmosphere and carbon isotopes the most slowly equilibrated, the renewal time for other substances (CO_2, NO_3, SiO_2, . . .) will lie in between the water and carbon-isotope renewal times.

15.7 Ventilation of the Main Oceanic Thermocline

The GEOSECS program has provided for the first time a reasonably detailed coverage of the distribution in the ocean of the ^{14}C and ^3H produced by nuclear testing. These distributions emphasize the importance of two phenomena evident but perhaps not fully appreciated through more conventional oceanographic observations. First they suggest an upwelling flux in the equatorial ocean comparable on a global scale to the flux of newly formed deep water (Broecker, Peng, and Stuiver, 1978). Second, they illustrate the importance of thermocline fronts located near lats. 15°N and 15°S (Broecker and Östlund, 1979).
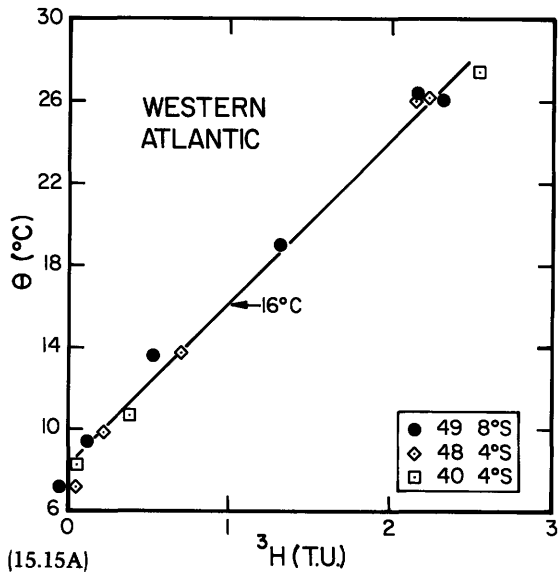
Strong upwelling in the equatorial ocean (or in the eastern boundary regions feeding into the equatorial zone) is suggested by the distribution of bomb-produced ^{14}C. The equatorial zone is characterized by low

surface-water bomb $^{14}C/C$ ratios and shallow penetration of bomb ^{14}C (relative to the adjacent temperate gyres). If the gas-invasion rate (from the atmosphere) into equatorial waters is comparable to that into temperate waters (as I believe it must be), then the low inventory of bomb ^{14}C in the equatorial zone can only be maintained by the input to the equatorial zone of water deficient in bomb ^{14}C. The only source of such water is upwelling from depths of at least 500 m. As the bomb ^{14}C distribution *within the equatorial zone* is quite homogeneous along isopycnal surfaces (figure 15.15), this isotope is not a sensitive indicator of the place at which upwelling occurs. However, by combining ^{14}C data with data for tracers like P_{CO_2}, P_{N_2O}, NO_3, NO_2, which have shorter surface-water response times than does ^{14}C, it may be possible to get at the entry pattern of upwelled water. Furthermore, time series of ^{14}C (as measured directly on water samples and as reconstructed through measurements of coral-growth rings) may reveal fluctuations in the rate of upwelling.

The distributions of ^{90}Sr and ^3H in the Atlantic demonstrate a front near 15°N, because the water-column inventory of these isotopes drops by an order of magnitude near that latitude. As shown in figure 15.16, the concentration of tritium along any given isopycnal also drops by an order of magnitude from north to south across this front (Broecker and Östlund, 1979). One reason for this difference is that the bulk of the ^{90}Sr and ^3H "fallout" occurred to the north of the equator. This asymmetry between hemispheres does not explain, however, why the boundary is so abrupt and why it lies near 15°N.

An answer to this dilemma comes from the equatorial upwelling inferred in the zone over which the thermocline is thin and shallow (i.e., 15°N to 15°S). As this upwelling is driven by the poleward divergence of equatorial surface water, any ^3H or ^{90}Sr reaching the equatorial zone by fallout or by leakage across the 15°N front will be pulled back to the surface and carried poleward across the front. Thus upwelling accounts for both the location of the fallout front and its sharpness.

As shown by Broecker et al. (1978), the distribution of ^{14}C in the equatorial zone yields a ratio of the flux of upwelled water to the invasion rate of CO_2. Since the latter has been independently determined, the upwelling flux can be obtained. Using this approach we obtained a flux of about 15×10^6 m³ s⁻¹ for the Atlantic equatorial zone. A preliminary analysis of the Pacific Ocean ^{14}C data suggests that the upwelling flux there is about 30×10^6 m³ s⁻¹. As mentioned above, no firm statement can yet be made as to where this upwelling occurs, for a high rate of lateral mixing obscures its origin.

W. S. Broecker

Figure 15.15A (left chart)

30

26   WESTERN
      ATLANTIC

22

Θ (°C)

18   ←16°C

14

10   ● 49 8°S
                ◇ 48 4°S
                □ 40 4°S
6

0   1   2   3
(15.15A)   ³H (T.U.)

Figure 15.15B (right charts)

30

26   WESTERN
      ATLANTIC   REF. LINE

22

θ (°C)

18   PRE-
     NUCLEAR   ←16°C

14

10   ● 49 8°S
                ◇ 48 4°S
6   □ 40 4°N

-100   0   100   150
          Δ¹⁴C(‰)

---

30   ✳

26   EASTERN   ✳
      ATLANTIC

22   REF. LINE

θ (°C)

18   PRE-   ←16°C
     NUCLEAR

14

10   ● 113 11°N
                ✳ 111   0°
6   ○ 107 12°S

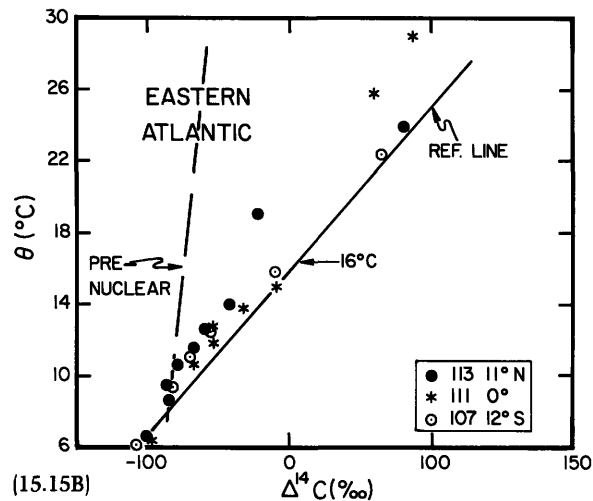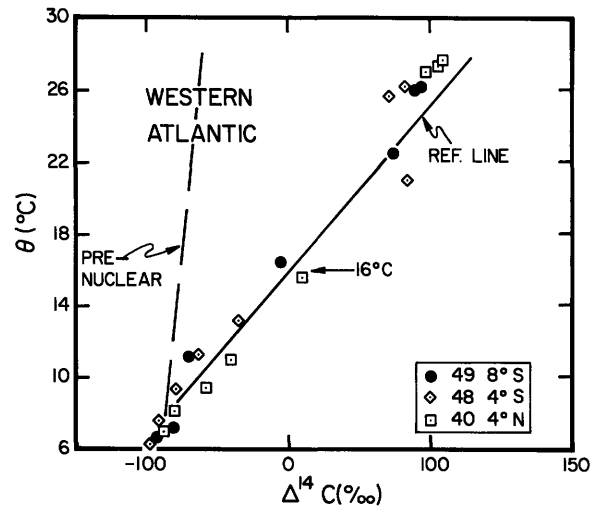-100   0   100   150
(15.15B)   Δ¹⁴C(‰)

Figure 15.15 Plots of tritium (A) and of radiocarbon (B) v. potential temperature in the equatorial thermocline of the Atlantic Ocean. The tritium data give the impression that tritium-bearing surface water is being mixed down into tritium-free water of potential temperature about 8°C. If 8°C water is taken to be the source for upwelling, then the ¹⁴C data can be interpreted as a mixture of surface water of $\Delta^{14}C = 100‰$ and 8°C water with a $\Delta^{14}C$ value of about $-90‰$.

15.8 Formation of Deep Waters

As pointed out, there are serious difficulties in using the distribution of natural radiocarbon to obtain deep-water formation rates. In the Antarctic this stems from the fact that the ¹⁴C clock is not reset during the formation process. In the deep Atlantic the anomaly due to radiodecay is small compared to the anomaly due to mixing. Also, there is no simple way to separate the contributions of the three (or possibly more) northern water types contributing to North Atlantic Deep Water. It behooves us therefore to seek other geochemical methods to gauge these fluxes. One obvious approach is to use the substances added to the ocean as a by-product of man's activities to trace recently formed deep water. The GEOSECS ³H section along the western basin in the Atlantic (figure 15.17) shows that the pathway followed by the newly formed water was in 1972 clearly "stained" with fallout products. So the potential is there. At a minimum, surveys spaced at decade intervals would clearly demonstrate the manner and rate at which the front of tritiated water is pushing its way into the western basin of the Atlantic.

The problem of inverting distributions of these transient tracers into fluxes is a difficult one. The geometry of the system is complex. Simple box-model representations are bound to give misleading answers. I do not mean to imply by this that the situation is hopeless. Rather the job will be a long one, requiring imagination, diligence, and excellent measurements.

It will be helpful, moreover, to explore what limitations the relationships among these tracers place on the types of dynamic models that might be employed. An example drawn from the GEOSECS observations will serve to illustrate this point. Despite quite differ-
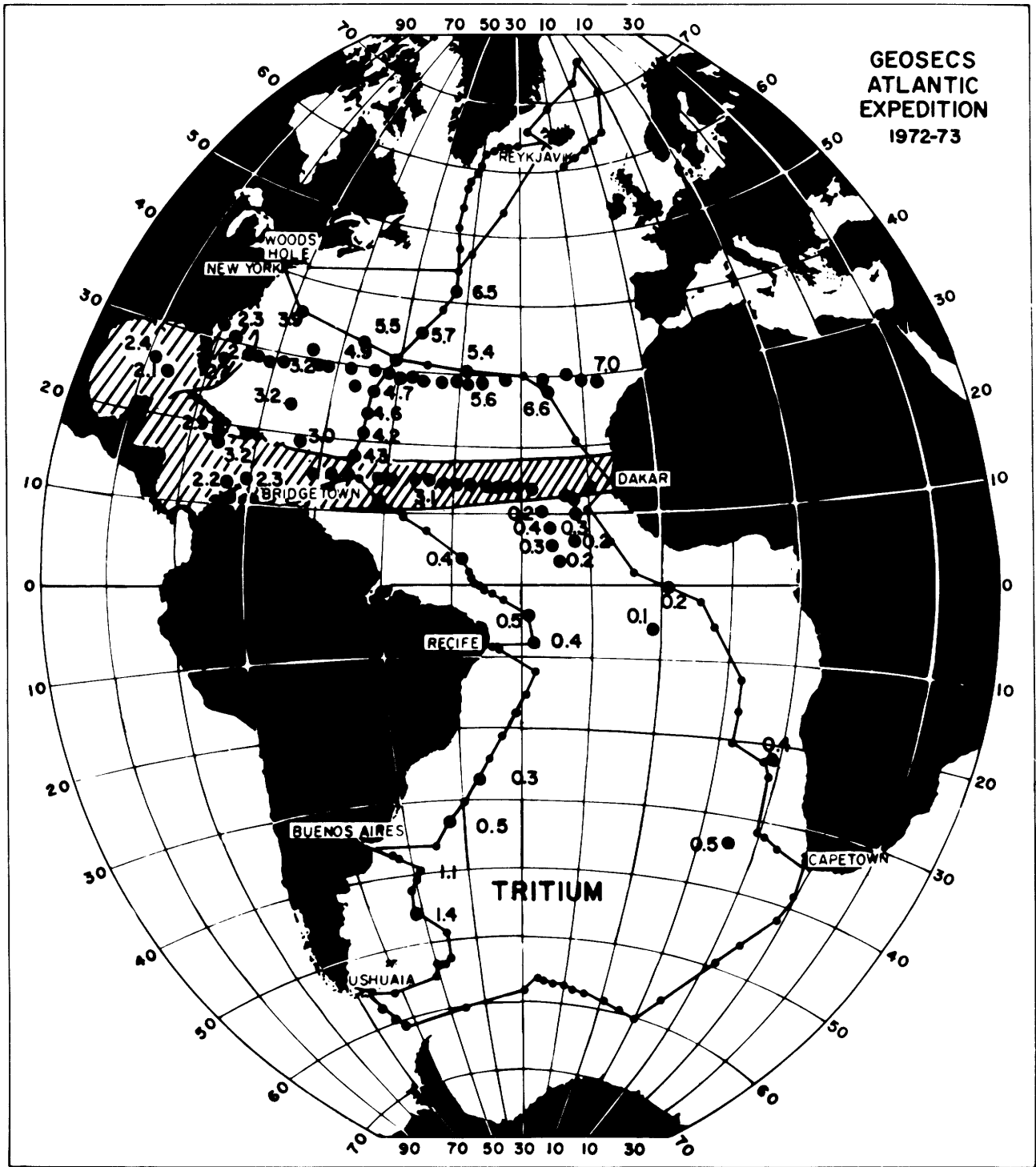
Figure 15.16 Tritium distribution along the isopycnal of $\sigma_\theta = 26.80$ in the Atlantic Ocean. The 15°N thermocline front constitutes a very pronounced boundary between high-tritium waters to the north and low-tritium waters to the south.

W. S. Broecker

ent input mechanisms, bomb-produced ^{14}C and ^{3}H show a very high degree of covariance in the northern Atlantic (figure 15.18). The samples included in this diagram cover the entire range of depth, geographical location, and water type. Modeling shows that different combinations of advection (away from the source region) and diffusion predict a great variety of ^{14}C-^{3}H trends. Thus the combined tracer fields can perhaps tell us not only the pathways followed but also something of the dynamics of the water movement.

15.9 Vertical Mixing Rates

Although there is no way to demonstrate how the isotopes we study penetrate into the interior of the ocean, we can still use their distributions to place upper limits on the rate of vertical mixing in the sea. This can be done by matching any given depth profile to a one-dimensional model, as has been carried out for profiles of ^{222}Rn and ^{228}Ra in the deep sea, and for profiles of

bomb ^{3}H and ^{14}C in the main oceanic thermocline, as shown in figure 15.19. The apparent vertical diffusivities obtained in this way show an inverse correlation with density gradient (Sarmiento et al., 1976; Hoffert and Broecker, 1978). Quay, Broecker, Hesslein, and Schindler (1980), using tritium injections into two small lakes in Canada, were able to obtain vertical diffusivities for much higher density gradients. As the tracers were allowed to spread laterally over the entire breadth of each lake, these results are true rather than apparent vertical diffusivities. As shown in figure 15.19, the tracer results from the lakes fall close to the extension of the oceanic curve.

It is difficult, however, to assess the significance of these results. Sarmiento and Rooth (1980) have shown that the bottom ^{222}Rn results could be explained entirely by mixing along isopycnals. Sarmiento (1978) has shown this to be the case for ^{228}Ra in the deep sea as well. It has long been suspected by oceanographers that the main thermocline of the ocean
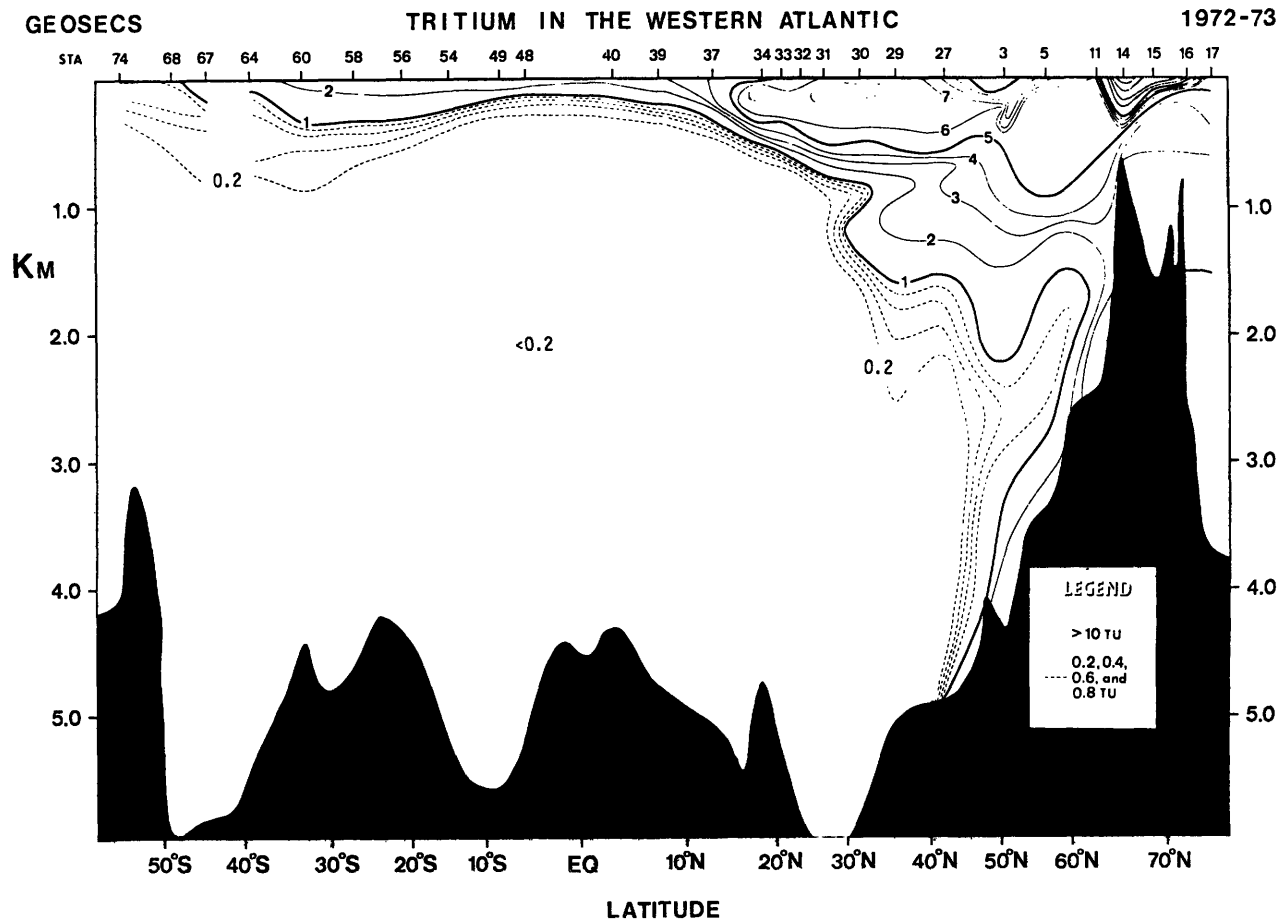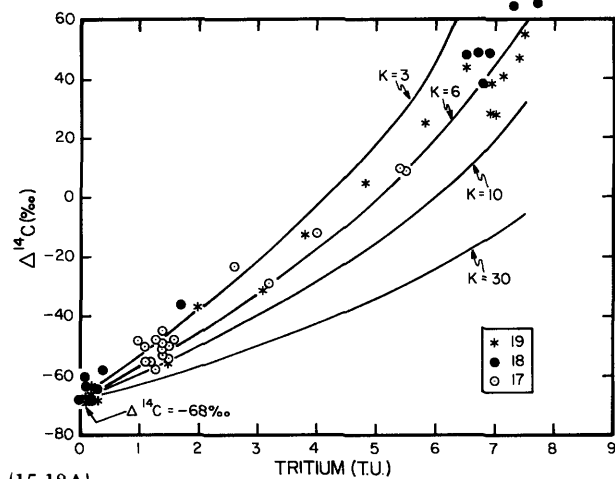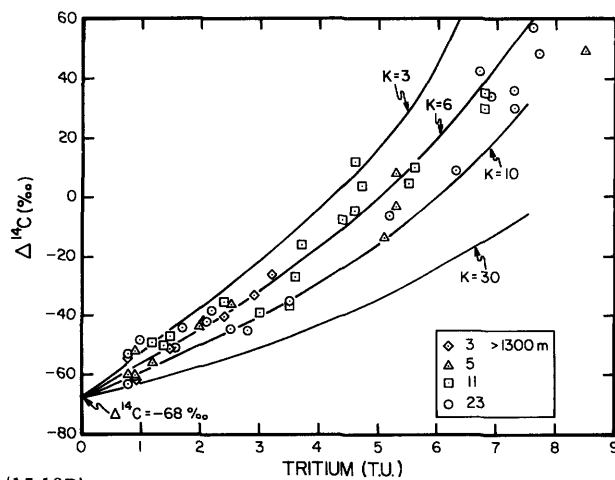

Figure 15.17 Tritium section along the western basin of the North Atlantic, prepared by Östlund of the University of Miami, who made all the tritium measurements for the GEOSECS program.

(15.18A)

(15.18B)

Figure 15.18 Tritium (in T.U.) vs. radiocarbon (in $\Delta^{14}C$) for water samples (from all depths) in the Norwegian Sea (A) and northern Atlantic (B). The solid curves show the results predicted by a one-dimensional diffusion model (the diffusion coefficients are in the units $cm^2\,s^{-1}$).
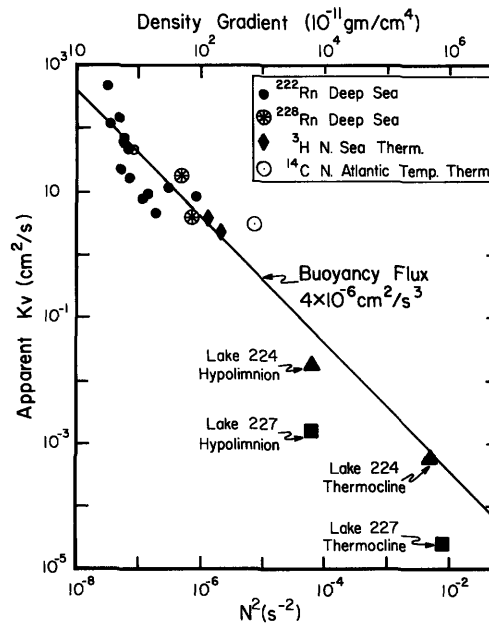

Figure 15.19 Apparent eddy diffusion coefficients for vertical mixing as measured by ^{222}Rn and ^{228}Ra in the deep sea (Sarmiento et al., 1976), ^{3}H in the pycnocline of the Norwegian Sea (Hoffert and Broecker, 1978) and bomb ^{14}C in the Sargasso Sea (Broecker et al., 1978) as a function of density gradient. Also shown are the results of Quay et al. (1980), obtained by tritium injections into small lakes.

is ventilated mainly along isopycnal surfaces. Certainly the distributions of bomb-produced ^{3}H and ^{14}C in the main oceanic thermocline could be explained by this process. The ^{7}Be profile shown above could be interpreted as an artifact of winter convection. Perhaps an argument relating to the angle between isopycnal surfaces and the tracer source (sea surface or floor) can be made as an alternative to the correlation between apparent vertical diffusivity and density gradient.

In my estimation the only way in which the relative importance of vertical and horizontal mixing can be established is to perform tracer injections at various points in the ocean interior. Such experiments (using ^{3}He as a tracer) would be comparable in cost to that for the large ocean science projects currently underway. The technology needed is available. By following a ^{3}He or tritium addition to an isopycnal horizon for several years, it would surely be possible to obtain a better estimate than we now have for the relative magnitudes of mixing along and perpendicular to isopycnal horizons. A knowledge of the relative importance of these processes is critical to the development of adequate models for the interpretation of radioisotope tracer data.